AM-BASEBAND TELEMETRY SYSTEMS

Volume 2: Carrier Synthesis from AM Modulated Carriers

by

RICHARD S. SIMPSON
Professor of Electrical Engineering

and

WILLIAM H. TRANTER
Research Associate

June, 1969

TECHNICAL REPORT NUMBER 103-102

COMMUNICATION SYSTEMS GROUP

BUREAU OF ENGINEERING RESEARCH

UNIVERSITY OF ALABAMA UNIVERSITY, ALABAMA

AM-BASEBAND TELEMETRY SYSTEMS

Volume 2: Carrier Synthesis from AM Modulated Carriers

by

Richard S. Simpson
Professor of Electrical Engineering

and

William H. Tranter
Research Associate

Technical Report Number 103-102

Prepared for

National Aeronautics and Space Administration
Marshall Space Flight Center
Huntsville, Alabama

Under Contract Number

NAS8-20172

University of Alabama Project Number

22-6509

Bureau of Engineering Research
University of Alabama
University, Alabama
June, 1969

ABSTRACT

An analysis of coherent demodulation in a DSB/FM telemetry system, having demodulation carriers synthesized from the modulated data-signal zero crossings, is performed. The analysis concerns the perturbing effects of both tape recorder flutter and noise on various system elements. These perturbations are reflected into system error by consideration of demodulation phase errors.

ACKNOWLEDGEMENT

The authors would like to express their appreciation to the Telemetry Systems Branch, Marshall Space Flight Center, for the support of this work. In particular, Mr. Walter O. Frost and Mr. Frank H. Emens have contributed significantly to this work through the many discussions which were held at MSFC.

TABLE OF CONTENTS

LIST OF ILLUSTRATIONS

LIST OF SYMBOLS

ω	frequency in radians per second
ω_m	modulating frequency
ω_n	Channel n carrier frequency
ω_N	phase-lock-loop natural frequency
ω_i	instantaneous frequency
ω_{nU}	instantaneous frequency of channel filter input (upper sideband component)
ω_{nL}	instantaneous frequency of channel filter input (lower sideband component)
$e_d(t)$	demodulated output
$e_{sc}(t)$	synthesized demodulation carrier
$e_{in}(t)$	input waveform
$e_{out}(t)$	output waveform
$e_{VCO}(t)$	VCO output
$e_v(t)$	VCO input
$e_\phi(t)$	phase detector output
$e_{\phi 1}(t)$	phase detector 1 output
$e_{\phi 2}(t)$	phase detector 2 output
$e_{DSB}(t)$	double-sideband signal
$e_{SSB}(t)$	single-sideband signal
$e_n(t)$	Channel n signal
$e_2(t)$	VCO output phase shifted 90 degrees
$e_{QDSB}(t)$	quadrature double-sideband signal
$e_{cfU}(t)$	upper-sideband portion of channel filter output
$e_{cfL}(t)$	lower-sideband portion of channel filter output

$e_{cf}(t$	channel filter output
$e_{nU}(t$	upper-sideband portion of channel filter input
$e_{nL}(t$	lower-sideband portion of channel filter input
$e_r(t)$	tape recorder input
$e_p(t)$	tape recorder output
S	Laplace operator
S_p	slope of channel filter phase characteristic
$F(S)$	loop filter of phase-lock loop
A_L	phase-lock-loop amplifier gain
A	total loop gain of phase-lock loop
a	phase-lock-loop filter parameter
ζ	damping constant
ρ	signal-to-noise ratio
Δ	monostable multivibrator duty cycle
$m(t)$	modulation signal
$x(t)$	nonlinear-network input
$y(t)$	nonlinear-network output
$n(t)$	additive noise
$c(t)$	carrier signal
$g(t)$	flutter
g_{peak}	peak value of $g(t)$
$h(t)$	time-base error
K_d	phase-detector constant
K_{VCO}	VCO constant
K_p	phase step magnitude
$2\psi(t)$	tracking error of PLL
$R(t)$	envelope of signal plus noise

$\phi(t)$	phase deviation of the channel carrier due to noise
$\theta(t)$	phase deviation of the channel carrier due to flutter
$\dot{\phi}(t)$	frequency deviation of the channel carrier due to noise
$\dot{\theta}(t)$	frequency deviation of the channel carrier due to flutter
$\dot{\theta}_{peak}$	peak value of $\theta(t)$
$\theta_e(t)$	phase error
$\theta_i(t)$	phase-lock loop input
$\theta_o(t)$	phase-lock loop output
θ_p	peak phase error
$\theta_m(t)$	envelope approximation of $\theta_o(t)$
y, x	dummy variables
z_m	average number of zero crossings per second of modulating signal
k	integer
α	modulating signal bandwidth
f_n	channel n carrier frequency in Hertz
P(SP)	probability of a shifted pulse
P(PDO)	probability of pulse dropout
p(x)	probability density of
σ	standard deviation
β_n	weighting functions
B	noise bandwidth
f_{PDO}	frequency above which PDO occurs
ξ	normalizing parameter for normal distribution
T_c	carrier period
T_o	value of $T_c/2$ below which PDO occurs
δ_k	k'th MSMV trigger

I. INTRODUCTION

AM baseband systems offer an efficient means for telemetering wideband data such as that which results from vibration or acoustic noise measurements. However, efficient power utilization requires that the AM modulation be of the suppressed carrier type. This implies that demodulation carriers must be synthesized from the information contained in the baseband. This process requires careful attention if the synthesized demodulation carrier is to have the proper phase relationship at the demodulator.

The process of carrier synthesis may be performed in two basic ways. The first method requires that a pilot be transmitted along with the baseband. This pilot may then be multiplied or divided to the frequency required for demodulation.[1] The second method involves operating upon a DSB signal in some manner such that a component is generated at some harmonic of the channel carrier frequency. This component may then be divided down to form the required demodulation carrier. In this report the second method is discussed in general and a particular demodulation carrier synthesis scheme, applicable only to a DSB channel, is investigated theoretically.

All carrier synthesis systems are adversely affected when the baseband is perturbed by noise or tape recorder flutter. These perturbations will be investigated as well as the effect of modulation zeros. The manner in which the synthesized demodulation carrier is affected by these perturbations is examined by a study of their effect on the phase error of the synthesized demodulation carrier.

---

[1] Superscripts refer to numbered references.

II. CARRIER SYNTHESIS FROM AM MODULATED CARRIERS

When the baseband of an AM/FM telemetry link contains DSB channels the carriers necessary for demodulation may be constructed from the individual DSB signals. There are many methods for doing this, several of which are investigated in this section.

A. Squaring

One of the simplest methods of generating the carrier component from a DSB signal is to pass the signal through a nonlinear network and then filter the component at the network output which is harmonically related to the required carrier frequency. As an example of this process consider the DSB signal

$$e_{DSB}(t) = m(t) \cos \omega_n t \ , \tag{2.1}$$

which is applied to a nonlinear network whose output, y(t), is given by

$$y(t) = \beta_1 x(t) + \beta_2 x^2(t) + \beta_3 x^3(t) + \beta_4 x^4(t) + \cdots \ , \tag{2.2}$$

where x(t) represents the input. For this case x(t) is $e_{DSB}(t)$ so that upon substitution of (2.1) into (2.2), y(t) becomes

$$\begin{aligned} y(t) = {} & \beta_1 m(t) \cos \omega_n t + \frac{\beta_2}{2} m^2(t) \left[1 + \cos 2 \omega_n t \right] + \\ & \frac{\beta_3}{4} m^3(t) \left[3 \cos \omega_n t + \cos 3 \omega_n t \right] + \\ & \frac{\beta_4}{8} m^4(t) \left[3 + 4 \cos 2 \omega_n t + \cos 4 \omega_n t \right] + \cdots \ . \end{aligned} \tag{2.3}$$

Since $m^k(t)$ is always positive for k an even integer, $m^k(t)$ has a nonzero dc value and consequently components are always present at the frequencies $k\omega_n$ for k even. One of these components may then be extracted and divided

down to the required carrier frequency. The extraction may be accomplished by a narrow bandwidth filter such as a phase-lock loop (PLL) or by use of a scheme which will be discussed in a following section.

There are two general problems which result when this method of carrier synthesis is used. They will be illustrated by assuming the nonlinear network to be a square law device, i.e.,

$$\beta_n = \begin{cases} 0 & n \neq 2 \\ 1 & n = 2 \end{cases} .$$

For this special case

$$y(t) = e^2_{DSB}(t) = \frac{1}{2} m^2(t) + \frac{1}{2} m^2(t)\cos 2\omega_n t . \tag{2.4}$$

The second term in (2.4) is equivalent to a carrier, $\cos 2\omega_n t$, amplitude modulated by a signal $\frac{1}{2} m^2(t)$. Since $m^2(t)$ has a nonzero dc value, the modulation is not suppressed carrier, i.e., a carrier component is present at $2\omega_n$.

The first problem is that if m(t) is zero, the DSB signal vanishes, and the carrier synthesis system ceases to operate, resulting in a loss of the demodulation carrier. When the modulation, m(t), again becomes nonzero, the carrier synthesis system takes a finite time to restore the demodulation carrier, and during this acquisition time, data may be lost. One method of correcting this problem is to place a pilot on each channel having a frequency higher than the highest modulation frequency as shown in Figure 2-1(a). The DSB signal for this case would be

$$e_{DSB}(t) = \left[\cos \omega_p t + m(t)\right] \cos \omega_n t , \tag{2.5}$$

a signal having components at $\omega_n + \omega_p$ and $\omega_n - \omega_p$ independent of the modulation. Thus, if m(t) becomes zero, the carrier synthesis system can still

operate, The main difficulty with this approach lies in the pilot position relative to the modulation spectrum, since the pilot must be removed from the data in the demodulator. If the pilot is placed too close to the data spectrum, the filtering problem for removing the pilot becomes difficult. Placing the pilot at higher frequencies results in poor spectrum utilization because of the bandwidth requirements. Spectrum utilization becomes quite important when a large number of channels are frequency multiplexed to form a baseband, as illustrated in Figure 2-1(b).

The second problem arises because the carrier is formed from its second harmonic. This gives rise to a phase ambiguity in the synthesized carrier because the initial phase of the synthesized carrier may be in error by π radians if only second harmonic information is available. Mathematically, this may be seen in the following manner. If cos ωt is squared the result is

$$\cos^2 \omega t = \frac{1}{2} + \frac{1}{2} \cos 2\omega t \ , \tag{2.6}$$

and squaring $\cos \left[\omega t + \pi \right]$ yields

$$\begin{aligned} \cos^2 \left[\omega t + \pi \right] &= \frac{1}{2} + \frac{1}{2} \cos \left[2\omega t + 2\pi \right] \\ &= \frac{1}{2} + \frac{1}{2} \cos 2\omega t \end{aligned} \tag{2.7}$$

which is an identical result. Thus, given the signal

$$e^2(t) = \frac{1}{2} + \frac{1}{2} \cos 2\omega t \tag{2.8}$$

there is no way of exactly determining e(t) without additional information.

It should be noted that a phase ambiguity exists in any system in which the demodulation carrier is derived by dividing some harmonic of the carrier. The type of ambiguity depends upon which harmonic is used to generate the demodulation carrier. As we have seen, using the second harmonic led to a situation where two initial phases of the fundamental gave

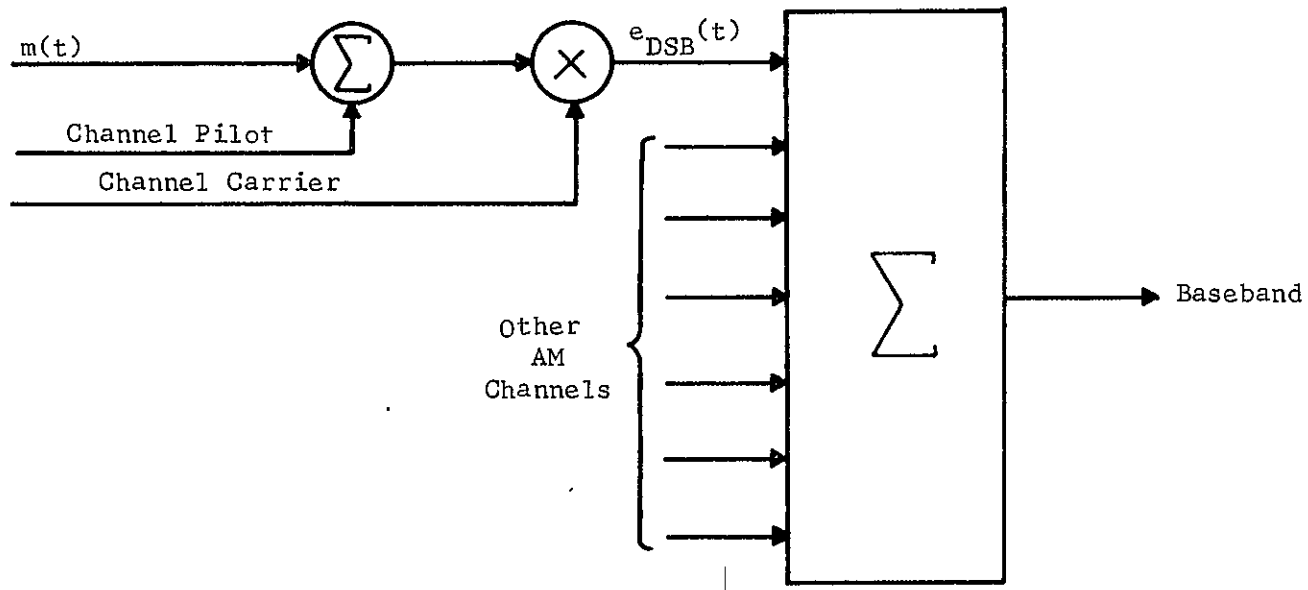

(a) Baseband Construction

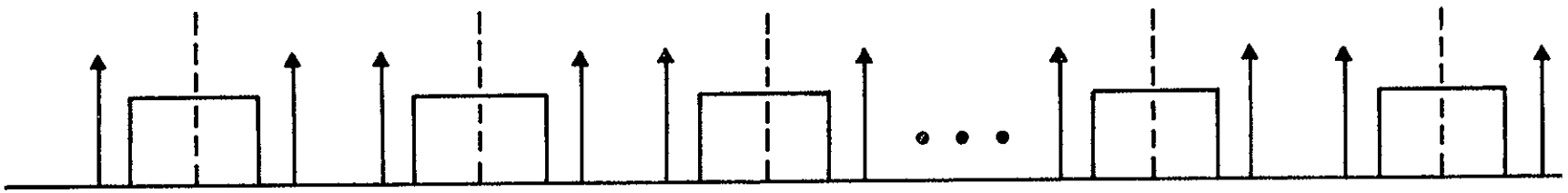

(b) Baseband Spectrum

Figure 2-1 AM-Baseband Formation

the same second harmonic. Four different phases will give the same fourth harmonic, and so on. Thus, the higher the harmonic used for synthesis, the more difficult ambiguity resolution becomes. This ambiguity must be removed prior to demodulation.

B. Costas Demodulator

The Costas demodulator[2], often referred to as the Costas or quadrature phase-lock loop (PLL), is a scheme in which a DSB signal is demodulated with a carrier generated by tracking the sidebands of the DSB signal with a voltage controlled oscillator (VCO). The Costas demodulator, actually a variation of the conventional PLL described in the Appendix, is illustrated in Figure 2-2.

In order to investigate the operation of the Costas demodulator, assume that the input to the loop is

$$e_{in}(t) = m(t) \cos \omega_n t \ , \tag{2.9}$$

where m(t) represents the modulation. The nominal VCO frequency is equal to the carrier frequency, ω_n, and its output may be expressed as

$$e_{VCO}(t) = \cos \left[\omega_n t + \theta_\varepsilon(t) \right] \ , \tag{2.10}$$

where $\theta_\varepsilon(t)$ is a time varying phase error. The action of the loop is to generate a signal proportional to $\theta_\varepsilon(t)$, which is then applied to the VCO input in order to correct the VCO phase. Thus, $\theta_\varepsilon(t)$ is driven to zero.

The manner in which this is accomplished is easily seen. The output of the first phase detector is $\left[e_{in}(t)\ e_{VCO}(t) \right]$ with the high frequency term filtered out. Now

$$e_{in}(t)\ e_{VCO}(t) = \tfrac{1}{2} m(t) \cos \omega_n t \cos \left[\omega_n t + \theta_\varepsilon(t) \right] \tag{2.11}$$

or

$$e_{in}(t)\ e_{VCO}(t) = \frac{1}{2} m(t) \left[\cos\ \theta_\varepsilon(t) + \cos \left[2\omega_n t + \theta_\varepsilon(t) \right] \right] \tag{2.12}$$

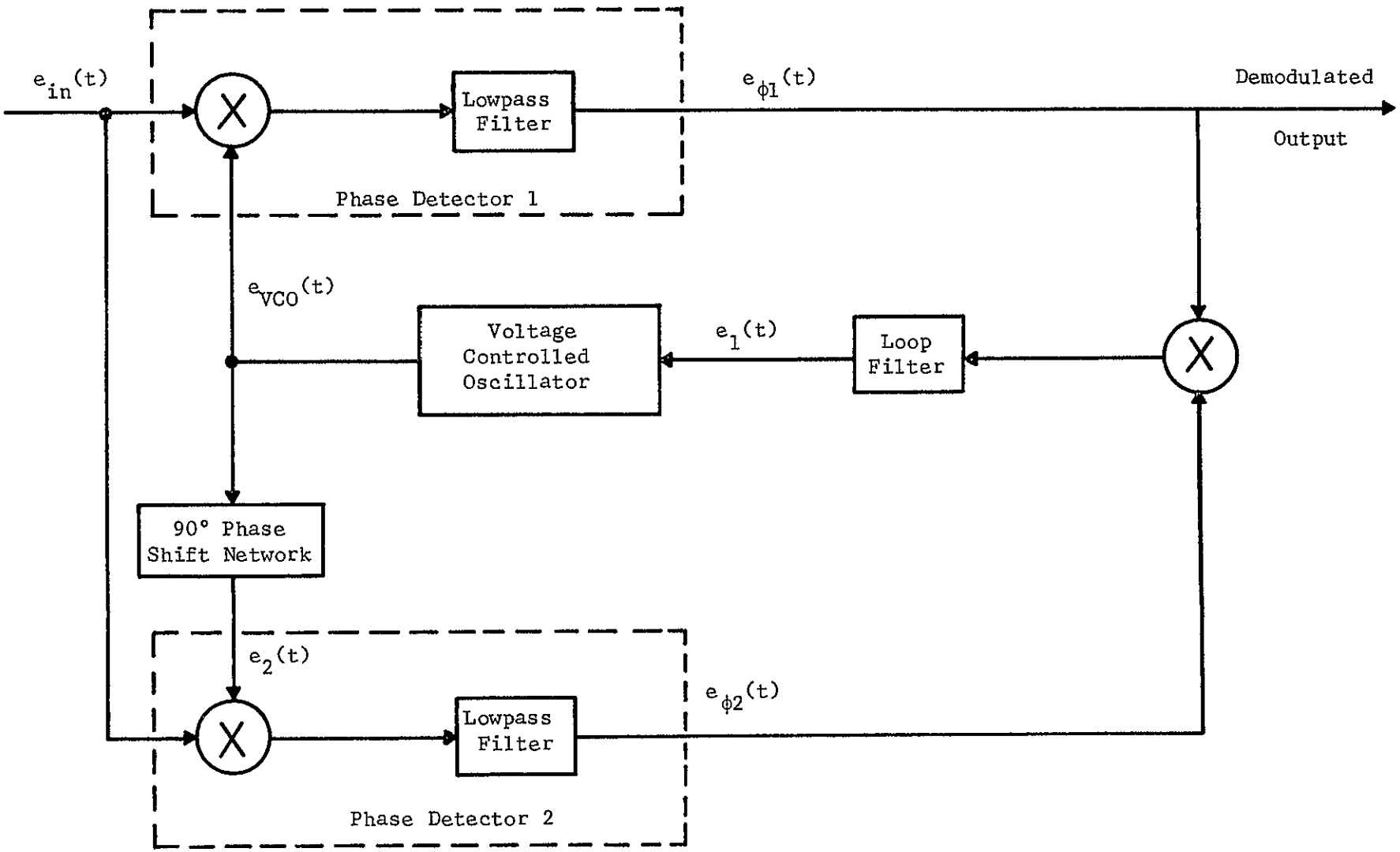

Figure 2-2 Costas Demodulator

Thus

$$e_{\phi 1}(t) = \frac{1}{2} m(t) \cos \theta_{\varepsilon}(t) . \tag{2.13}$$

In the same manner, $e_{\phi 2}(t)$ is given by $\left[e_{in}(t)\ e_2(t)\right]$ with the high frequency term filtered out, where $e_2(t)$ is $e_{VCO}(t)$ shifted 90° in phase. Thus,

$$e_{in}(t)\ e_2(t) = m(t) \cos \omega_n t \sin \left[\omega_n t + \theta_{\varepsilon}(t)\right] \tag{2.14}$$

or

$$e_{in}(t)\ e_2(t) = \frac{1}{2} m(t) \left[\sin \theta_{\varepsilon}(t) + \sin \left[2\omega_n t + \theta_{\varepsilon}(t)\right]\right] \tag{2.15}$$

which yields

$$e_{\phi 2}(t) = \frac{1}{2} m(t) \sin \theta_{\varepsilon}(t) . \tag{2.16}$$

The output of the product device preceding the loop filter may be written as

$$e_{\phi 1}(t) e_{\phi 2}(t) = \frac{1}{8} m^2(t) \sin 2\theta_{\varepsilon}(t) , \tag{2.17}$$

which is

$$\frac{1}{8} m^2(t) \left[2\theta_{\varepsilon}(t)\right]$$

for small values of $\theta_{\varepsilon}(t)$. The phase error, $\theta_{\varepsilon}(t)$, is a slowly varying function of time, while $m^2(t)$ has much higher spectral content. The loop filter is a lowpass filter which ideally passes $\theta_{\varepsilon}(t)$ but not the modulation. Thus

$$e_1(t) = K\ \theta_{\varepsilon}(t) , \tag{2.18}$$

which controls the VCO in such a manner as to reduce $\theta_{\varepsilon}(t)$. Therefore, the output of the first phase detector is the demodulated output for the channel.

One disadvantage of this scheme is that modulating signals having near dc components are passed by the loop filter and adversely affect the

VCO control voltage. There are two other problems of interest, both of which also arose in the squaring scheme discussed earlier. These are phase ambiguity and the effect of zero modulation.

Equation (2.17) shows that the error control voltage is proportional to $\sin 2\theta_\varepsilon(t)$; thus the error voltage is the same for incremental changes in $\theta_\varepsilon(t)$ about zero as for incremental changes about π radians. This is equivalent to stating that a π radian phase ambiguity exists in the synthesized demodulation carrier. This results in an ambiguity in the polarity of the demodulated output. As with the squaring scheme, resolution of the ambiguity requires additional information.

Another problem is that if m(t) should go to zero and remain there for several cycles of the channel carrier, the input of the loop would fall to zero, and consequently the loop would cease operating properly. The loop would have to re-acquire lock when m(t) becomes nonzero, the result being lost data. This problem may be eliminated by using a pilot as discussed previously. If there were no modulation, the pilot signal would remain as an input to the Costas loop allowing continuous operation.

C. A Nonlinear Scheme Utilizing a Limiter and a Monostable Multivibrator

Since the output of a DSB modulator is given by the product of the modulation and carrier signals, the DSB signal has zero crossings at both the carrier and modulation zeros. The carrier necessary for demodulation may be synthesized from these zero crossings[3,4,5].

The demodulation system is illustrated in Figure 2-3. The channel filter selects the proper channel from the baseband spectrum. The output of the channel filter is the DSB signal to be demodulated and to be used for demodulation carrier synthesis. The operation of the carrier synthesis loop can be explained using Figure 2-4, which illustrates the waveforms present at various points in the loop.

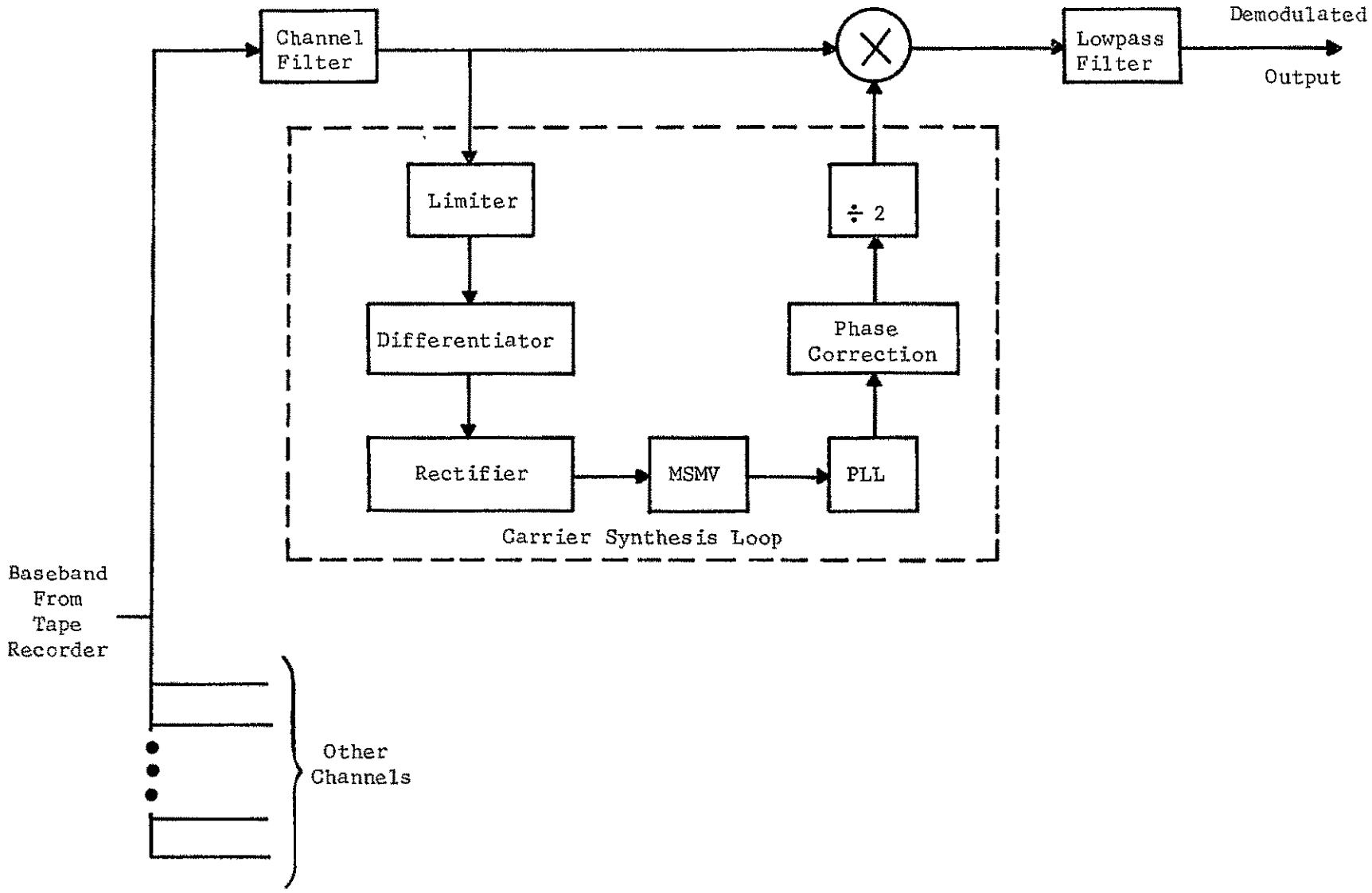

Figure 2-3 AM-Baseband Demodulator

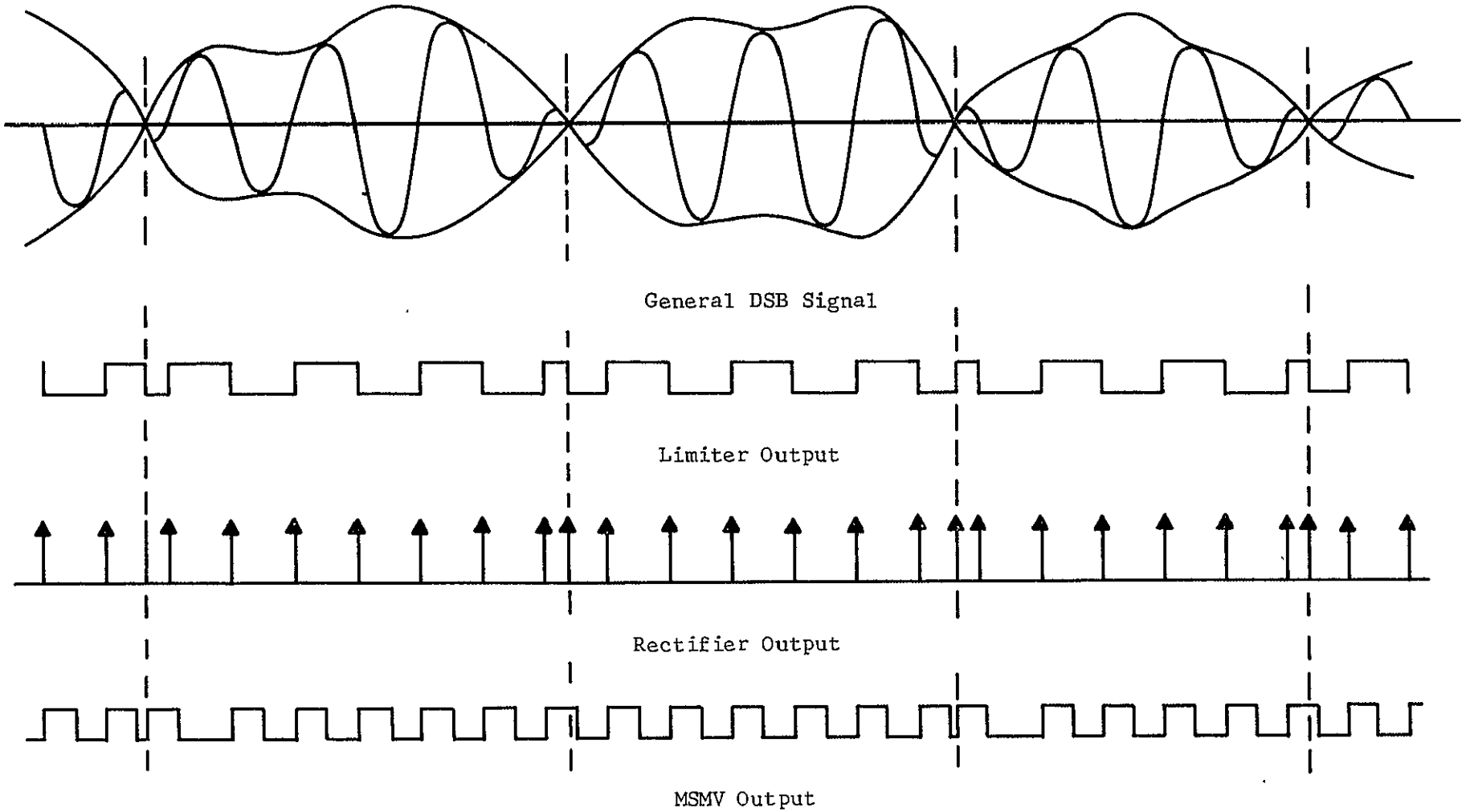

Figure 2-4 Generation of MSMV Output

The DSB signal is first amplitude limited to form a periodic pulse train. Differentiating this pulse train forms a series of impulse functions which mark the time of the carrier and modulation zero crossings. The full-wave rectifier gives all impulses a positive polarity and provides triggers for a monostable-multivibrator (MSMV) of duty cycle Δ, which is defined as

$$\Delta = \frac{\text{MSMV "on" time}}{\text{MSMV period}} \qquad (2.19)$$

The MSMV output is a pulse train having a nominal repetition rate equal to twice the channel carrier frequency.

The leading edges of the MSMV output exactly mark the time of the carrier zero crossings, except upon the occurrence of a modulation zero crossing. The modulation zero crossings perturb the MSMV output only when they occur during the MSMV "off" times. This perturbation, when present, takes the form of a MSMV pulse shifted to the right. If Δ is 0.5 or greater, no additional pulses may appear in the MSMV output.

Since perturbations result only when modulation zeros occur during the MSMV "off" time, the action of the MSMV is to eliminate the effect of a certain percentage of modulation zeros. This percentage is directly dependent upon Δ. Thus, if Δ is made arbitrarily large, no perturbations result from the modulation zeros. The result of this action will be discussed in Chapter IV.

The PLL is assumed to track the fundamental of the MSMV output pulse train. The signal formed, after phase correction and division by two, yields the demodulation carrier. The frequency division is necessary because of the fact that the MSMV is triggered twice every carrier period; thus, the MSMV fundamental frequency is twice the carrier frequency. The need for phase correction results from the inherent 90° phase shift in

the PLL, and the phase shift caused by the MSMV if Δ is different from 0.5. The action of the divide-by-two network will be discussed in the following chapter when a signal is carried through the carrier synthesis system to determine the effect of recorder flutter.

D. Signal Restrictions

In order for the zero-crossing synthesis scheme to operate properly, there must exist a one-to-one correspondence between the carrier zero crossings and the zero crossings of the signal present at the input to the carrier synthesis loop. Since a DSB signal is given by

$$e_{DSB}(t) = m(t)c(t) \ , \tag{2.20}$$

it is clear that zero crossings of both m(t) and c(t) yield zero crossings of $e_{DSB}(t)$. If the carrier frequency is much larger than the highest frequency contained in m(t), most of the zero crossings will be due to the carrier and the scheme will function properly. The effect of the zero crossings of m(t) will be investigated in Chapter IV.

The zero crossings of a single-sideband signal do not in general correspond to the carrier zero crossings. This may be seen by considering the signal

$$e_{SSB}(t) = \cos(\omega_n + \omega_m)t \ , \tag{2.21}$$

which is an SSB signal resulting from sinusoidal modulation, where ω_n and ω_m represent the carrier and modulating frequencies, respectively. This signal has zeros where

$$(\omega_n + \omega_m)t = (\frac{\pi}{2})(2k + 1) \tag{2.22}$$

for k an integer. Thus, $e_{SSB}(t)$ does not have zero crossings at the carrier zero crossings independent of the modulation; therefore, the demodulation carriers can not be synthesized from the SSB signal.

The same result holds for a quadrature DSB signal, $e_{QDSB}(t)$. This can be seen by writing

$$e_{QDSB}(t) = m_1(t) \cos \omega_n t + m_2(t) \sin \omega_n t \ , \tag{2.23}$$

where $m_1(t)$ and $m_2(t)$ are the modulating signals on the direct and quadrature carriers. The above expression may be written

$$e_{QDSB}(t) = \sqrt{m_1^2(t) + m_2^2(t)} \cos (\omega_n t + \phi) \ , \tag{2.24}$$

where

$$\phi = - \tan^{-1} \frac{m_2(t)}{m_1(t)} \tag{2.25}$$

Thus $e_{QDSB}(t)$ has zero crossings at

$$\omega_n t - \tan^{-1} \frac{m_2(t)}{m_1(t)} = \frac{\pi}{2} (2k + 1) \ , \tag{2.26}$$

where k is an integer. Thus, $e_{QDSB}(t)$ has no zero crossings independent of the modulation; therefore, the demodulation carriers cannot be synthesized from a quadrature multiplexed signal.

There are special cases where a demodulation carrier may be synthesized from a quadrature DSB signal. For example, when the spectra of one modulating signal has significant frequency content in a region where the spectra of the other modulating signal is zero, filtering may be utilized to yield a DSB signal. This is illustrated in Figure 2-5 for the case where $m_2(t)$ has no low frequency content. Filtering $e_{QDSB}(t)$ yields a DSB signal from which a demodulation carrier may be synthesized. When $m_1(t)$ and $m_2(t)$ have similar spectra, a pilot may be added to one of the signals. The pilot may then be filtered out to yield a DSB signal.

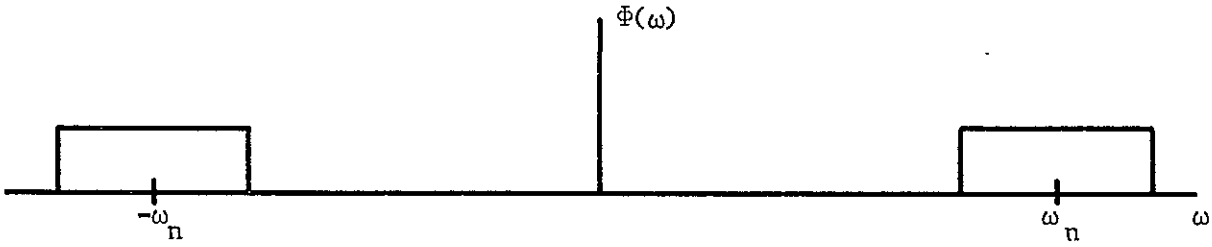

Spectra of $m_1(t) \cos \omega_n t$

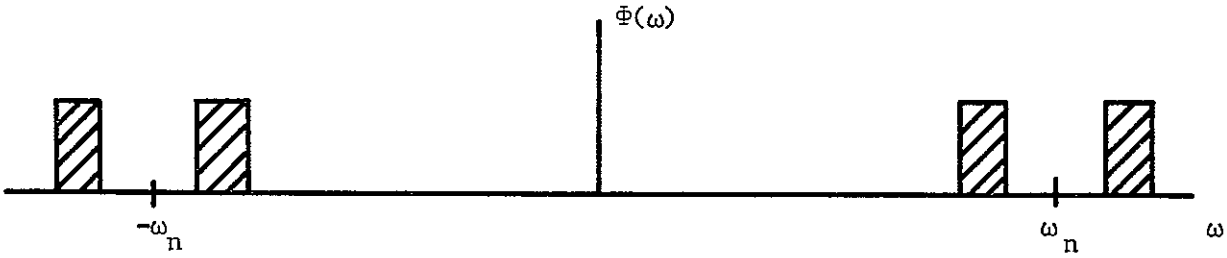

Spectra of $m_2(t) \sin \omega_n t$

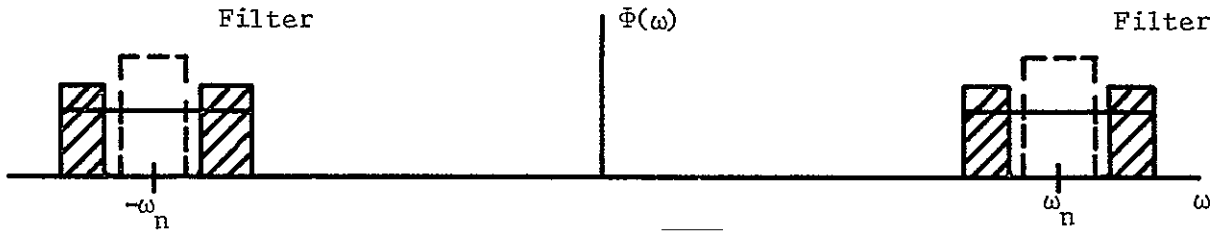

Spectra of $e_{QDSB}(t)$

(Filtering with a filter having the illustrated characteristic yields a DSB signal which can be used for synthesis.)

Figure 2-5 Carrier Synthesis from a Quadrature DSB Signal

III. EFFECT OF FLUTTER FOR SINUSOIDAL MODULATION

The carrier synthesis loop will now be analyzed to determine the effect of flutter upon sinusoidal modulation when the demodulation carrier is synthesized from the DSB modulated channel carrier, For purposes of this analysis modulation zeros and noise will be neglected; therefore, the zero crossings of the DSB signal will be identically the zero crossings of the carrier. The problem is then to determine the perturbations on the DSB signal due to flutter.

The major effect of flutter is to introduce a time-base error (TBE) in a recorded signal. Assuming the recorded signal is $e_r(t)$, the playback signal may be written

$$e_p(t) = e_r\left[t + h(t)\right] \tag{3.1}$$

where h(t) represents the composite TBE due to both the record and playback TBE. The validity of (3.1) depends upon the time derivative of TBE (or flutter) being small, which is the case for most recorders[6].

For ease of analysis, the channel pilots will be neglected so that the Ghannel n input to the channel filter (see Figure 2-3) may be written as

$$e_n(t) = \cos\left[(\omega_n + \omega_m)(t + h(t))\right] + \cos\left[(\omega_n - \omega_m)(t + h(t))\right] \tag{3.2}$$

$$e_n(t) = \cos\left[(\omega_n + \omega_m)t + (\omega_n + \omega_m)h(t)\right] \cos\left[(\omega_n - \omega_m)t + (\omega_n - \omega_m)h(t)\right] \tag{3.3}$$

Equation (3.3) indicates that the effect of TBE is to introduce in the signal being recorded a phase perturbation having a magnitude proportional to the frequency of the recorded signal. Equation (3.3) may be written in the form

$$e_n(t) = \cos\left[(\omega_n + \omega_m)t + \frac{\omega_n + \omega_m}{\omega_n}\theta(t)\right] + \cos\left[(\omega_n - \omega_m)t + \frac{\omega_n - \omega_m}{\omega_n}\theta(t)\right] \tag{3.4}$$

by making the definition

$$\theta(t) = \omega_n h(t) \ . \tag{3.5}$$

Thus, $\theta(t)$ represents the phase perturbation of the channel carrier due to flutter.

The signal given by (3.4) exists at the input of the channel filter, and the output of this filter is to be determined. The input has variable frequency because $\theta(t)$ is a time varying function. The output will be obtained by utilizing the steady-state transfer function evaluated at the instantaneous input frequency, ω_i. Such a solution is known as the quasi-steady-state, or quasi-stationary, solution[7] and may be expressed as

$$e_{out}(t) = e_{in}(t)H(\omega_i) \tag{3.6}$$

where

$e_{in}(t)$ = input signal,

$e_{out}(t)$ = output signal, and

$H(\omega_i)$ = network transfer function evaluated at the instantaneous input frequency.

The channel data filter will be assumed to have a linear phase characteristic, $\phi(\omega_i)$, as shown in Figure 3-1, and a unity amplitude characteristic

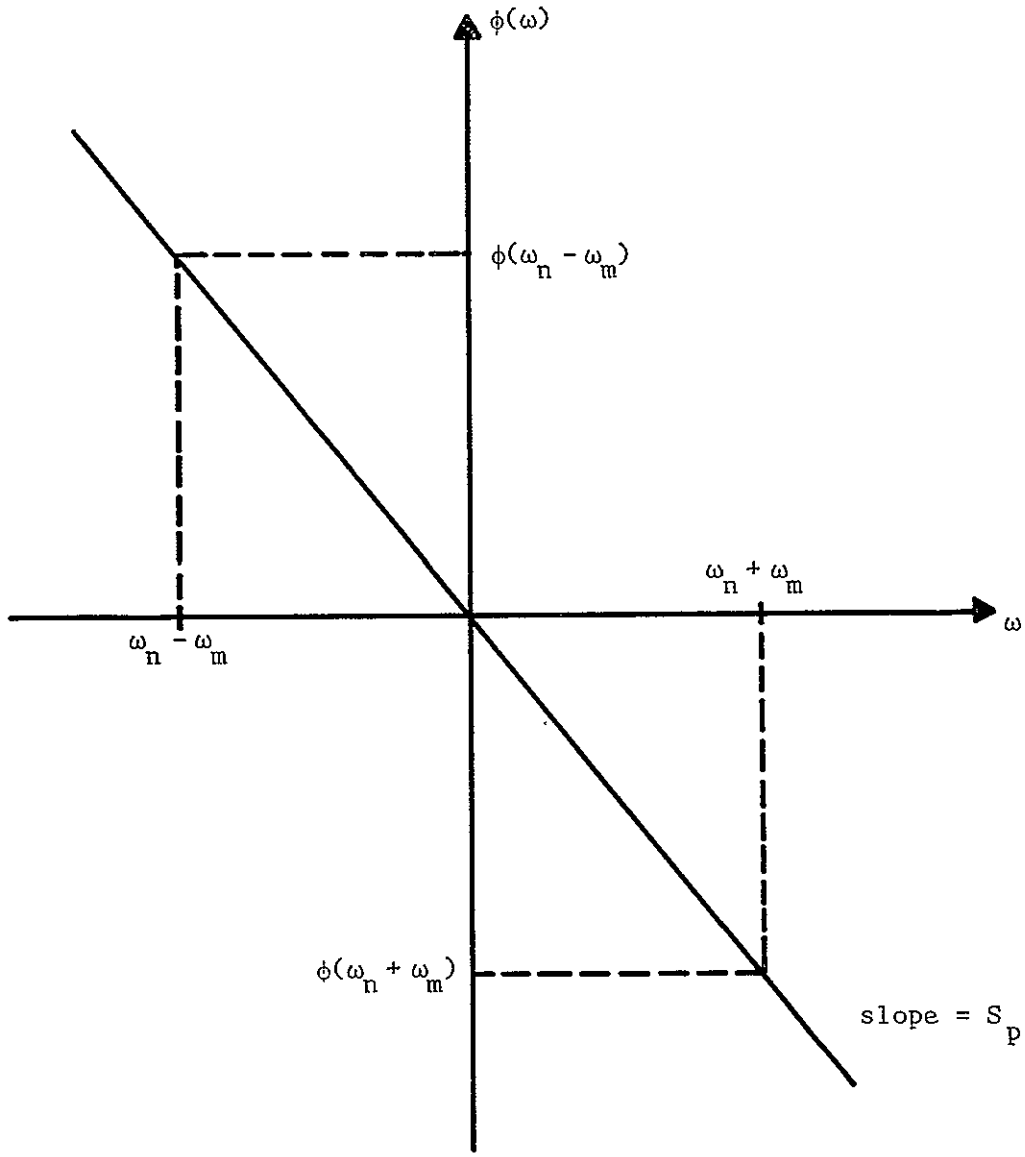

Figure 3-1 Channel Filter Phase Characteristic

over the range of interest. Thus,

$$H(\omega_i) = \phi(\omega_i) = \exp\left[j S_p(\omega_i - \omega_n)\right] \tag{3.7}$$

where S_p represents the slope of the data channel phase characteristic. For ease of analysis $e_n(t)$ is decomposed into upper and lower sidebands, $e_{nU}(t)$ and $e_{nL}(t)$, where

$$e_{nU}(t) = \text{Re exp } j\left[(\omega_n + \omega_m)t + \frac{\omega_n + \omega_m}{\omega_n}\theta(t)\right] \tag{3.8}$$

and

$$e_{nL}(t) = \text{Re exp } j\left[(\omega_n - \omega_m)t + \frac{\omega_n - \omega_m}{\omega_n}\theta(t)\right] \tag{3.9}$$

The instantaneous frequencies of $e_{nU}(t)$ and $e_{nL}(t)$ are

$$\omega_{nU} = (\omega_n + \omega_m) + \frac{\omega_n + \omega_m}{\omega_n}\dot{\theta}(t) \tag{3.10}$$

and

$$\omega_{nL} = (\omega_n - \omega_m) + \frac{\omega_n - \omega_m}{\omega_n}\dot{\theta}(t) \ , \tag{3.11}$$

respectively. The upper-sideband output of the channel filter, $e_{cfU}(t)$, can then be written as

$$e_{cfU}(t) = e_{nU}(t)H(\omega_{nU}) \ , \tag{3.12}$$

which is

$$e_{cfU}(t) = \text{Re}\left[\exp j\left[(\omega_n + \omega_m)t + \frac{\omega_n + \omega_m}{\omega_n}\theta(t)\right]\times \exp j\left[S_p\omega_m + S_p\frac{\omega_n + \omega_m}{\omega_n}\dot{\theta}(t)\right]\right] \tag{3.13}$$

or

$$e_{cfU}(t) = \cos\left[(\omega_n + \omega_m)t + \frac{\omega_n + \omega_m}{\omega_n}\theta(t) + S_p\omega_m + S_p\frac{\omega_n + \omega_m}{\omega_n}\dot{\theta}(t)\right] \tag{3.14}$$

The lower-sideband output may be determined in exactly the same manner and combined with $e_{cfU}(t)$ to yield the total channel filter output, which is

$$e_{cf}(t) = \cos\left[(\omega_n + \omega_m)t + \frac{\omega_n + \omega_m}{\omega_n}\theta(t) + S_p\omega_m + S_p\frac{\omega_n + \omega_m}{\omega_n}\dot{\theta}(t)\right] + \cos\left[(\omega_n - \omega_m)t + \frac{\omega_n - \omega_m}{\omega_n}\theta(t) - S_p\omega_m + S_p\frac{\omega_n - \omega_m}{\omega_n}\dot{\theta}(t)\right] \tag{3.15}$$

This is the signal which is to be demodulated, and the signal from which the demodulation carrier is to be synthesized.

The response of the carrier synthesis loop to $e_{cf}(t)$ is easily explained. The limiter removes all amplitude information from the filter output and retains only carrier and modulation zero crossings. The effect of modulation zero crossings on the carrier synthesis loop will be determined in the next chapter so that here ω_m will be assumed zero. Under this assumption, the input to the limiter is

$$2\cos\left[\omega_n t + \theta(t) + S_p\dot{\theta}(t)\right]$$

which has zero crossings at

$$\omega_n t + \dot{\theta}(t) = \frac{(2k+1)\pi}{2}\ , \tag{3.16}$$

where k is an integer. Thus, the leading edges of the MSMV output pulses occur at

$$\omega_n t + \theta(t) + S_p\dot{\theta}(t) = \frac{(2k+1)\pi}{2} \tag{3.17}$$

Figure 3-2 illustrates three zero crossings of the carrier and consequently three MSMV output pulses. The MSMV duty cycle, Δ, is 0.50 in the illustration; therefore the positive going zero crossings of the MSMV fundamental frequency are coincident with the channel carrier of the zero crossings. If Δ is not 0.50, then the zero crossings of the MSMV fundamental

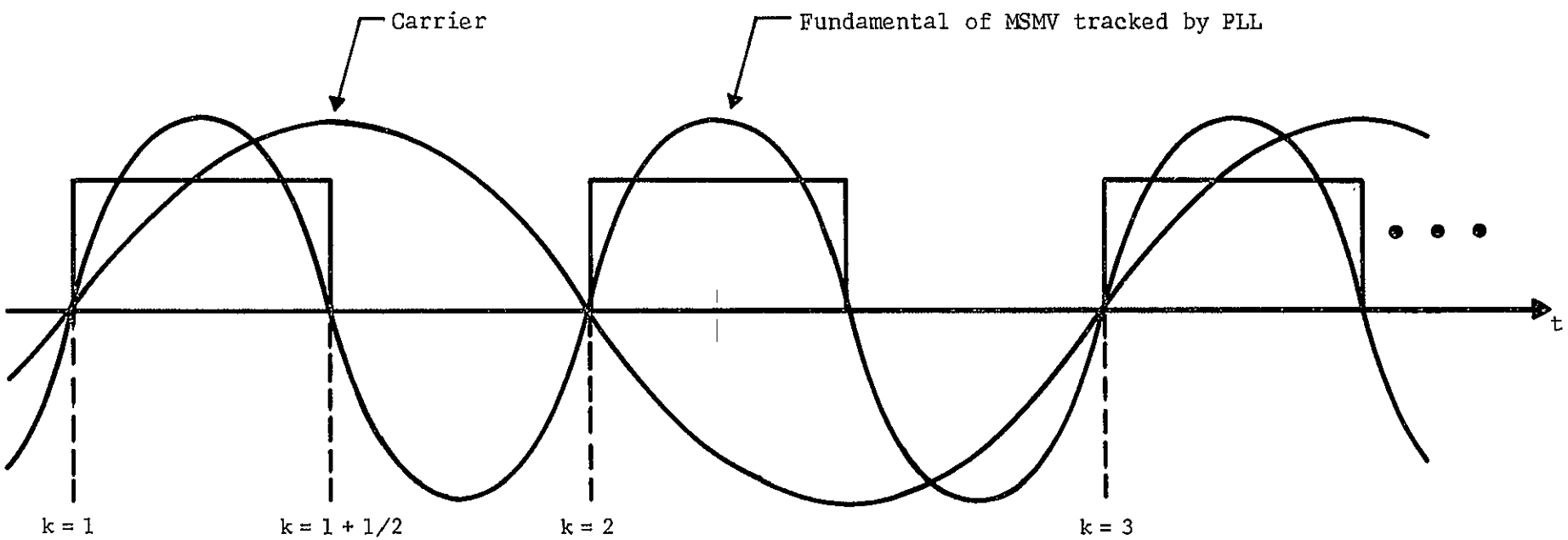

Figure 3-2 MSMV Output

are offset by a fixed value, which may be compensated in the phase correction network following the PLL. Assuming that the PLL bandwidth is sufficiently large to track the phase perturbation due to tape recorder flutter, the PLL output will be the input shifted by 90° as shown in the Appendix. This 90° phase shift may also be compensated by the phase correction network. Thus, assuming perfect tracking, the output of the phase correction network will be the MSMV fundamental, which has zero crossings for integral values of k as well as other zero crossing corresponding to $k + 1/2$. Thus, the output of the divide-by-two network is

$$e_{sc} = \cos \left[\omega_n t + \theta(t) + S_p \dot{\theta}(t) \right] \tag{3.18}$$

which is the demodulation carrier.

The action of the divide-by-two network deserves comment since it is the source of a 180° phase ambiguity similar to the ambiguity which exists in the squaring process and in the Costas demodulator. The source of this ambiguity is in the rectification process, which doubles the fundamental frequency. The result is illustrated in Figure 3-3. The zero crossings of the divider input corresponding to integral values of k are easily determined, since the divider input has positive slope at these points. However, there are two possible carriers which may be derived from the divider input. This results in a 180° phase ambiguity in the synthesized demodulation carrier, and consequently, a polarity ambiguity in the demodulated output.

Multiplying (3.15) and (3.18) and filtering the components centered at $2\omega_c$ yields

$$\underset{\text{(A)}}{} \quad \underset{\text{(B)}}{} \quad \underset{\text{(C)}}{} \quad \underset{\text{(D)}}{}$$

$$e_d = \cos \left[\omega_m t + \omega_m \theta(t) + S_p \omega_m + S_p \omega_m \dot{\theta}(t) \right] \tag{3.19}$$

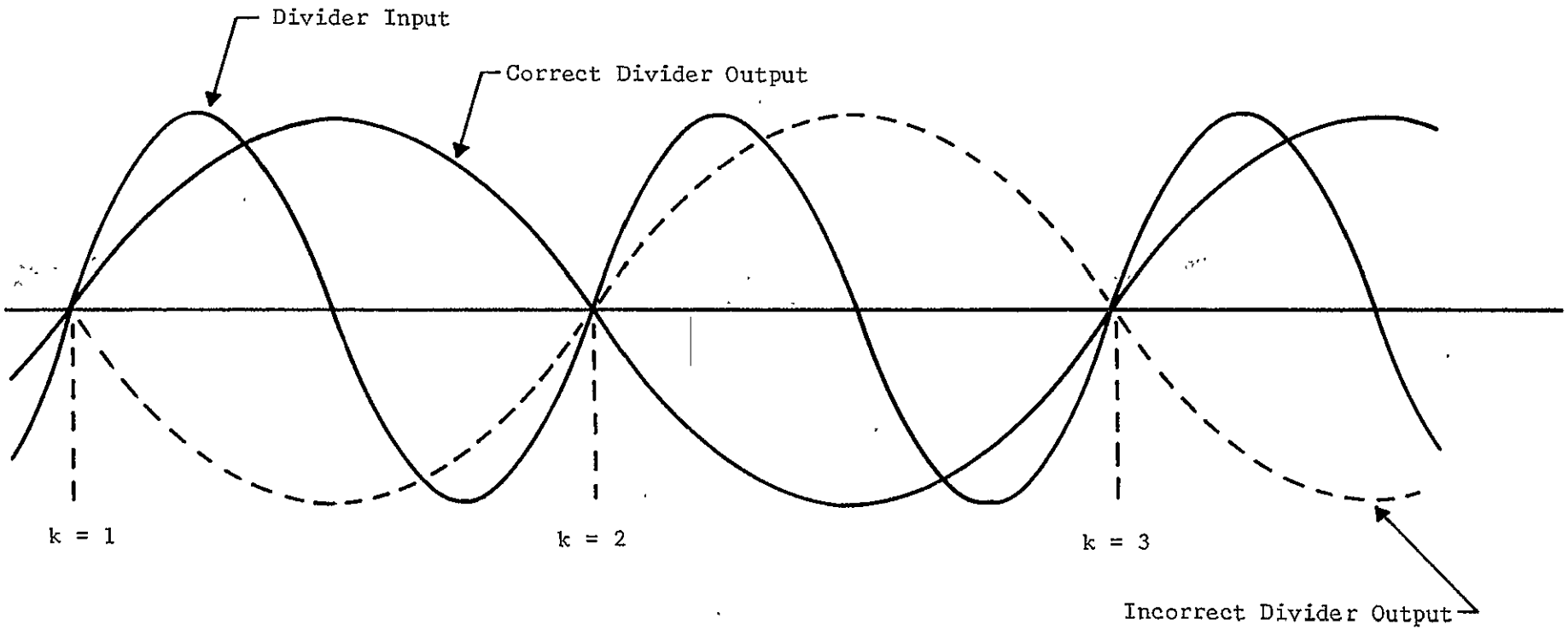

Figure 3-3 Source of Phase Ambiguity

for the demodulated output. Terms (A) and (B) yield no distortion, since (A) is the desired term and (B) is a linear phase shift arising from the envelope delay of the channel filter. Term (C) is a distortion term which arises from TBE in the data, and it would appear if the data were recorded and played back directly, i.e., if there were no modulation-demodulation process involved. Term (D) results from the interaction of the data filter and the flutter. Data taken on several older records indicates that Term (B) is much more significant than Term (D).

Equation (3.19) is developed assuming perfect tracking of the PLL. If the bandwidth of the PLL is too small, tracking error results. If $2\psi(t)$ is the phase error of the PLL due to tracking error, the demodulated output is given by

$$e_d(t) = \cos\psi(t)\ \cos\left[\omega_m t + \omega_m \theta(t) + S_p \omega_m + S_p \omega_m \dot{\theta}(t)\right] \qquad (3.20)$$

System accuracy of 1% dictates that $\psi(t)$ must not exceed approximately 8 degrees. As will be shown in the following chapter, when noise is present in the carrier synthesis loop, the PLL bandwidth should be made as small as possible. With typical recorders, a PLL bandwidth of 200-500 Hz offers a good compromise.

IV. OTHER PERTURBING EFFECTS

In addition to tape recorder flutter, which will be present independent of the technique used to synthesize the demodulation carrier, there are other perturbations present in the demodulation scheme illustrated in Fig. 2-3. The most notable of these are perturbations resulting from modulation zeros, perturbations of the MSMV due to noise and flutter, and perturbations of the phase-lock loop output due to channel noise.

A. Modulation Zeros

An understanding of the mechanism by which modulation zeros affect the carrier synthesis scheme can be obtained from Figure 2-4. The limited DSB signal is a periodic pulse train except in the region of a modulation zero crossing. When the limiter output is differentiated and rectified, a series of impulses are formed, which trigger the MSMV. The MSMV output consists of a pulse train whose leading edges correspond to the carrier zero crossings except for the pulses perturbed by modulation zeros. Observation reveals that modulation zeros result in shifted pulses when they occur during the MSMV "off" time and have no effect otherwise. The shift is always in the same direction, and the PLL responds to these pulses in a manner dependent upon the loop bandwidth. If the loop bandwidth is sufficiently large, significant phase errors in the demodulation carrier can result.

The probability that a pulse in the MSMV output will be shifted is of interest. If we consider the modulating waveform to have an "ideal" lowpass spectrum of bandwidth α Hz, the average number of zero crossings per second, z_m, may be written as[8]

$$z_m = 1.155\,\alpha \tag{4.1}$$

If the MSMV duty cycle, Δ, is 50 percent or greater, no additional pulses can be inserted in the MSMV output by modulation zeros, and the number of pulses per second in the MSMV output is constant at $2f_n$. Therefore, the probability of a shifted pulse, P(SP), is the ratio of perturbed pulses to total pulses in the MSMV output or

$$P(SP) = \frac{\text{Number modulation zeros}}{\text{Number of carrier zeros}} \quad \frac{\text{MSMV "off" time}}{\text{MSMV period}}$$

This yields

$$P(SP) = \frac{1.155\ \alpha}{2f_n}(1 - \Delta) \tag{4.2}$$

which is plotted in Figure 4-1 for three different values of the MSMV duty cycle.

It is necessary to examine the behavior of the PLL to determine the effect of a shifted pulse on the demodulation carrier. To accomplish this requires consideration of the statistics of the shifted pulse. A modulation zero has equal probability of falling anywhere in a carrier period. Therefore, the probability density function describing the time shift will be uniform from zero to the total "off" time, $(1 - \Delta)/2f_n$. The average time shift is therefore $(1 - \Delta)/4f_n$, which corresponds to a phase shift of $\pi(1 - \Delta)$ radians at $2f_n$.

The peak phase shift of the PLL output corresponding to a phase shift of an input pulse can be obtained by considering the perturbed pulse to be a phase step, of $1/2f_n$ duration, applied directly to the PLL. The amplitude of the pulse will be $\pi(1 - \Delta)$ radians. The PLL is assumed to have a response with exponential envelope, $\exp(-\zeta\omega_N t)$, where ζ is the loop damping and ω_N is the natural frequency as defined in the Appendix. This is the response of a first-order PLL. However, as shown in the Appendix, it may be used to approximate the envelope of the second-order PLL response

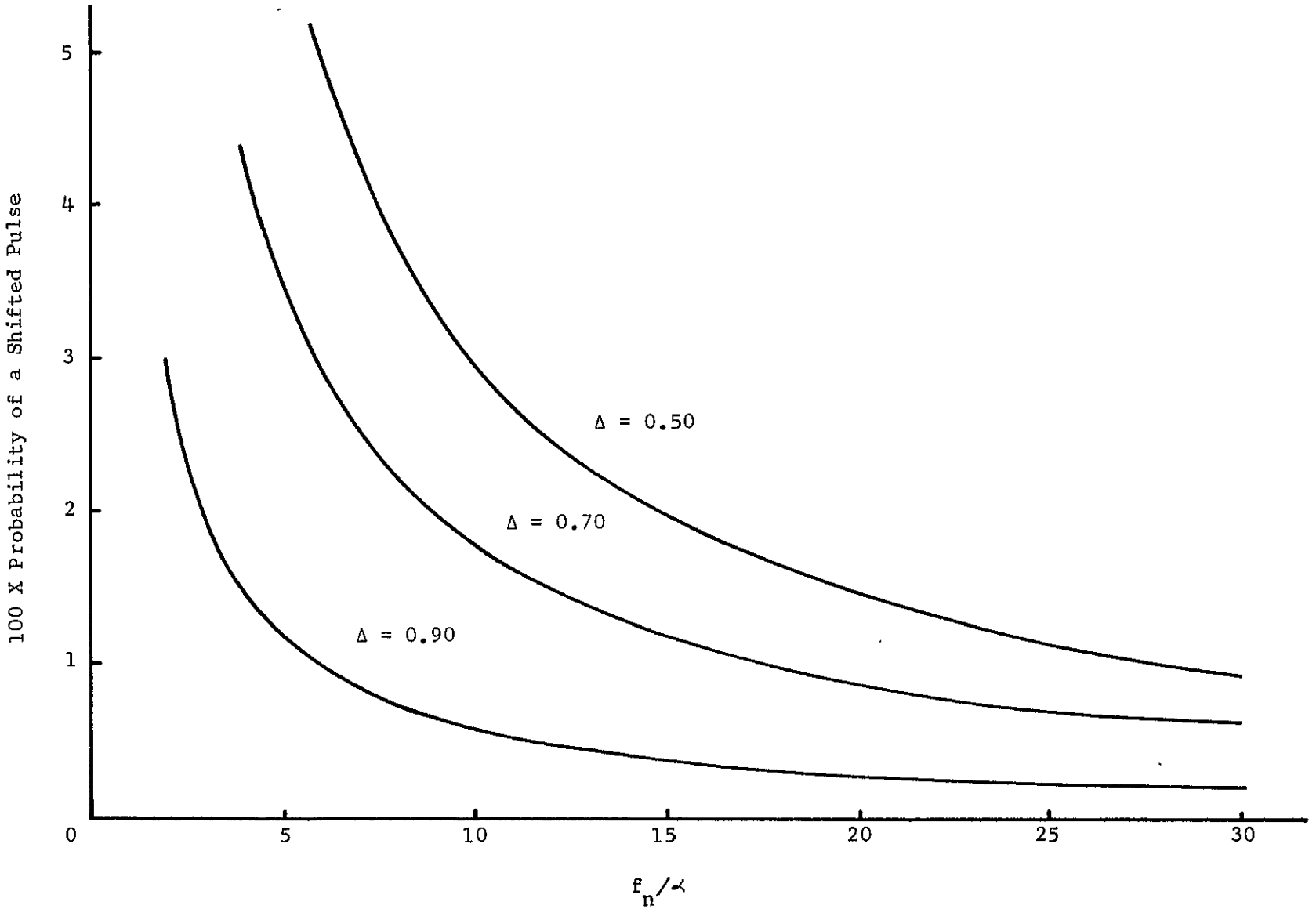

Figure 4-1 Probability of a Shifted Pulse

with a phase step as input. Therefore, the response to the pulse input may be approximated as

$$\theta_o(t) = \pi(1 - \Delta)(1 - e^{-\zeta\omega_N t}) \tag{4.3}$$

for

$$0 \leq t \leq 1/2f_n \ .$$

Thus, for the average phase shift, the peak phase error, θ_p, in the demodulation carrier at f_n is

$$\theta_p = \frac{\pi}{2}(1 - \Delta)(1 - e^{-\zeta\omega_N \frac{1}{2f_n}}) \ , \tag{4.4}$$

which is plotted in Figure 4-2 for $\zeta = 0.707$, $\omega_N = 2\pi(500)$, and several values of Δ. As the product $\zeta\omega_N$ increases, the PLL has less of a smoothing effect, and the peak phase errors become correspondingly higher. This analysis is based upon the linear model of the PLL and assumes that lock is maintained.

Figure 4-1 indicates that for reasonable values of f_n/α the probability of a shifted pulse is low. Figure 4-2 indicates when a shifted pulse does occur, the peak phase error for the average shift is small, particularly if the MSMV duty cycle and the carrier frequency are high. As a rough rule it is concluded that the effect of modulation zeros will be negligible, i.e., the peak phase error will be less than approximately three degrees if f_n is greater than 5α and 15 kHz and if Δ is greater than 70 percent.

B. Monostable Multivibrator Perturbations Due to Noise

Increasing Δ to minimize the effect of modulation zeros may add to other difficulties, the most important of which results from additive noise in the baseband. This difficulty may best be visualized by assuming the

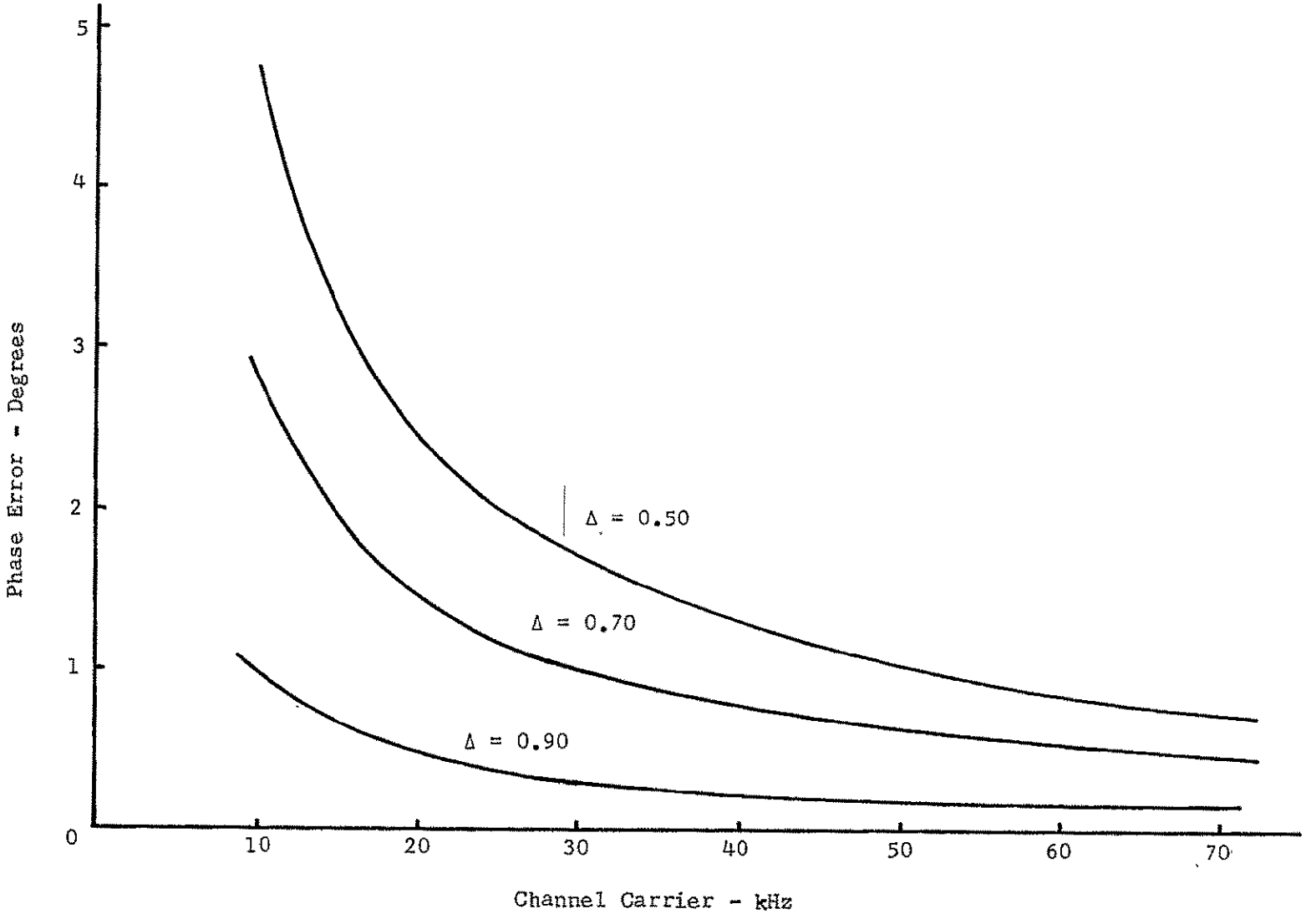

Figure 4-2 Peak Phase Error Due to Modulation Zeros

modulating signal to be constant at unity. Under this condition, the DSB signal becomes a sinusoid at the channel carrier frequency, ω_n. The input to the limiter may be written as

$$e_{cf}(t) = \cos\left[\omega_n t + n(t)\right] \tag{4.5}$$

where n(t) represents additive noise which is narrowband by virtue of the channel filter. Since n(t) is narrowband, (4.5) may be placed in the form

$$e_{cf}(t) = R(t)\cos\left[\omega_n t + \phi(t)\right] \tag{4.6}$$

where R(t) represents the envelope and $\phi(t)$ represents phase deviation due to noise. Both R(t) and $\phi(t)$ are slowly varying functions compared to ω_n. The quantity of interest is the instantaneous frequency

$$\omega_i = \omega_n + \dot{\phi}(t) \ . \tag{4.7}$$

The MSMV output pulse train is illustrated in Figure 4-3. The delta functions, δ_k, represent the MSMV triggers. As the instantaneous frequency increases due to an increase in $\dot{\phi}(t)$ resulting from noise, the zero crossings and hence the MSMV triggers move closer together. This effectively increases the MSMV duty cycle since the MSMV "on" time is fixed. This is illustrated in Figure 4-4.

At a particular point, the zero crossings are separated by an amount equal to the "on" time of the MSMV. Any increase in frequency above this value results in a condition called pulse dropout (PDO). This occurs when the trigger for a zero crossing falls at a time when the MSMV is in the "on" state. The frequency at which PDO first occurs is denoted f_{PDO}. From Figure 4-3

$$T_c = \frac{1}{f_n} \tag{4.8}$$

and

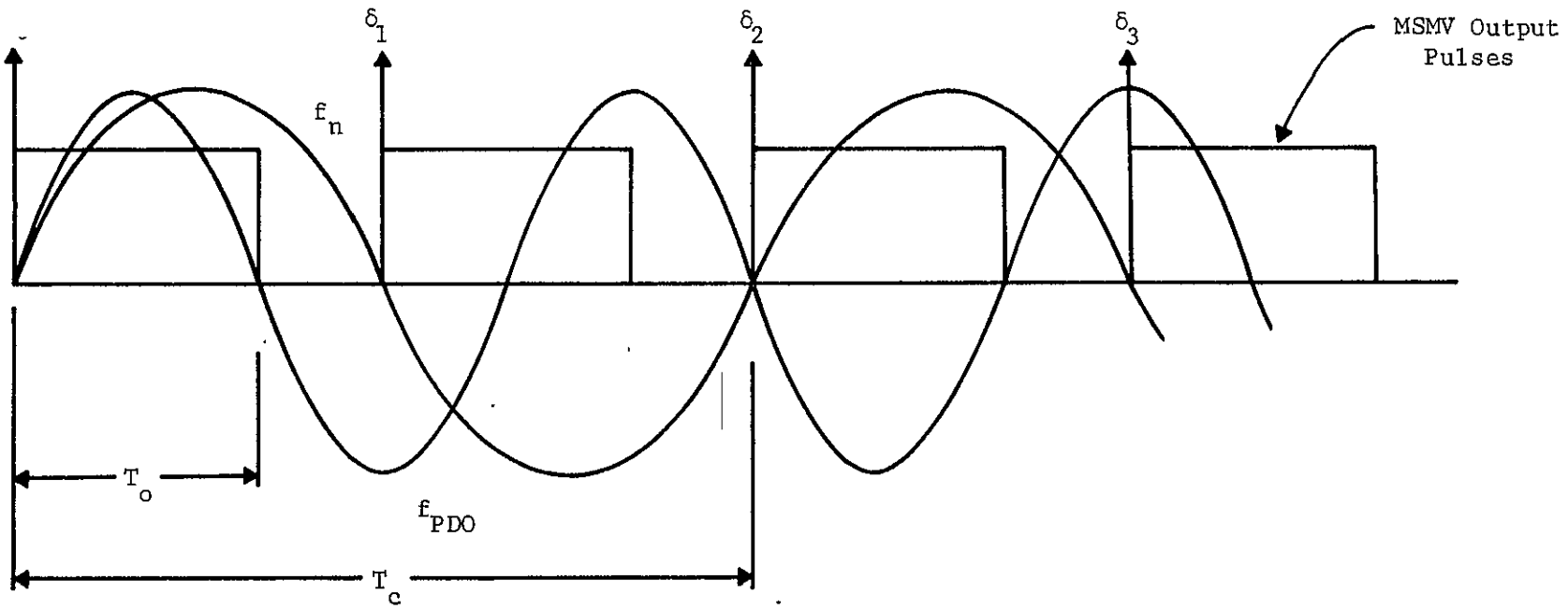

Figure 4-3 MSMV Output Illustrating the Frequency of Pulse Dropout

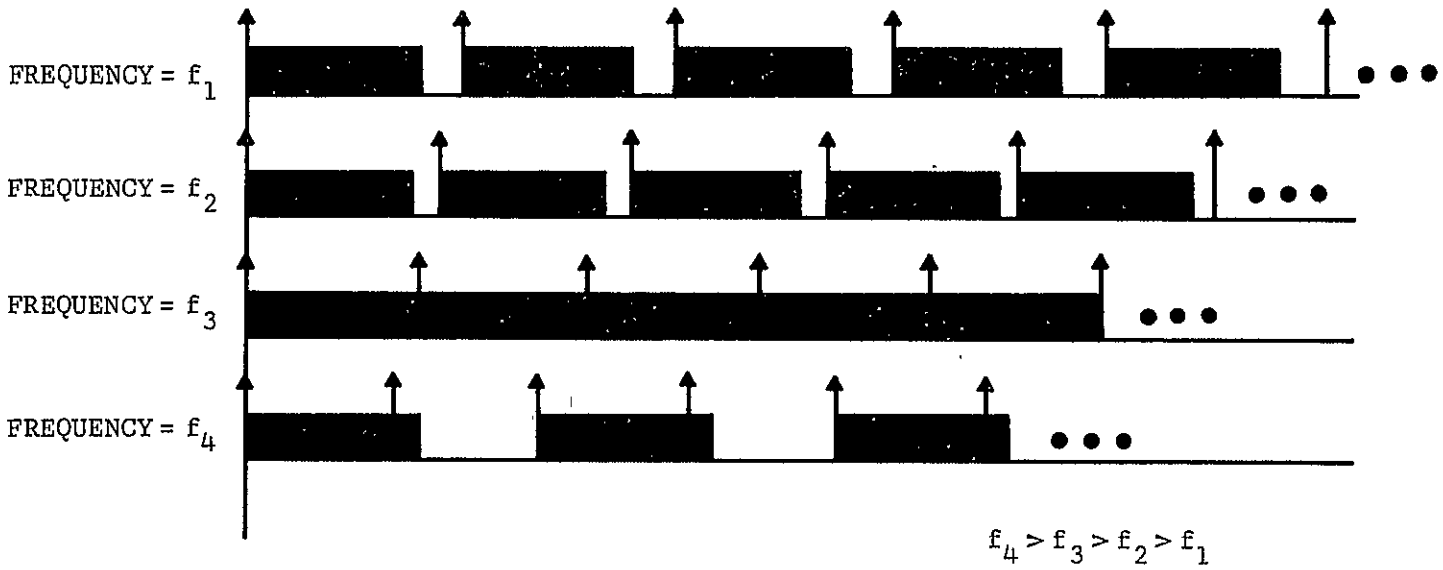

Figure 4-4 MSMV Output for Increasing Frequency Deviation

$$T_o = \Delta \frac{T_c}{2} = \frac{\Delta}{2f_n} \quad . \tag{4.9}$$

The frequency for PDO is given by

$$f_{PDO} = \frac{1}{2T_o} = \frac{f_n}{\Delta} \quad . \tag{4.10}$$

The instantaneous frequency in Hz is given by

$$f_i = f_n + \frac{1}{2\pi} \dot{\phi}(t) \tag{4.11}$$

which, at the threshold of PDO, becomes

$$\frac{f_n}{\Delta} = f_n + \frac{1}{2\pi} \dot{\phi}(t) \tag{4.12}$$

or

$$\dot{\phi}(t) = 2\pi f_n \left(\frac{1 - \Delta}{\Delta}\right) \quad . \tag{4.13}$$

Thus, PDO occurs when

$$\dot{\phi}(t) \geq 2\pi f_n \left(\frac{1 - \Delta}{\Delta}\right) \quad . \tag{4.14}$$

Since PDO can have an adverse effect on the PLL, such as causing it to lose lock, it is of interest to determine the probability of PDO, P(PDO), given f_n, Δ, and the noise statistics. Because of the complexity of the general analysis, this will be done only for dc modulation.

For dc modulation $e_{cf}(t)$ is a sine wave perturbed by additive, narrow-band, noise. S. O. Rice has developed a curve which yields the probability that $\dot{\phi}(t)$ is less than some particular value when the signal-to-noise ratio, ρ, and the noise bandwidth, B, are known.[9] Equation (4.14) may be used to adapt Rice's curve to the one illustrated in Figure 4-5.

Figure 4-5 illustrates that P(PDO) is highly dependent upon the ratio of the channel carrier frequency to the noise bandwidth, as would be expected. Thus, this effect is greatest in wideband, low-carrier-frequency

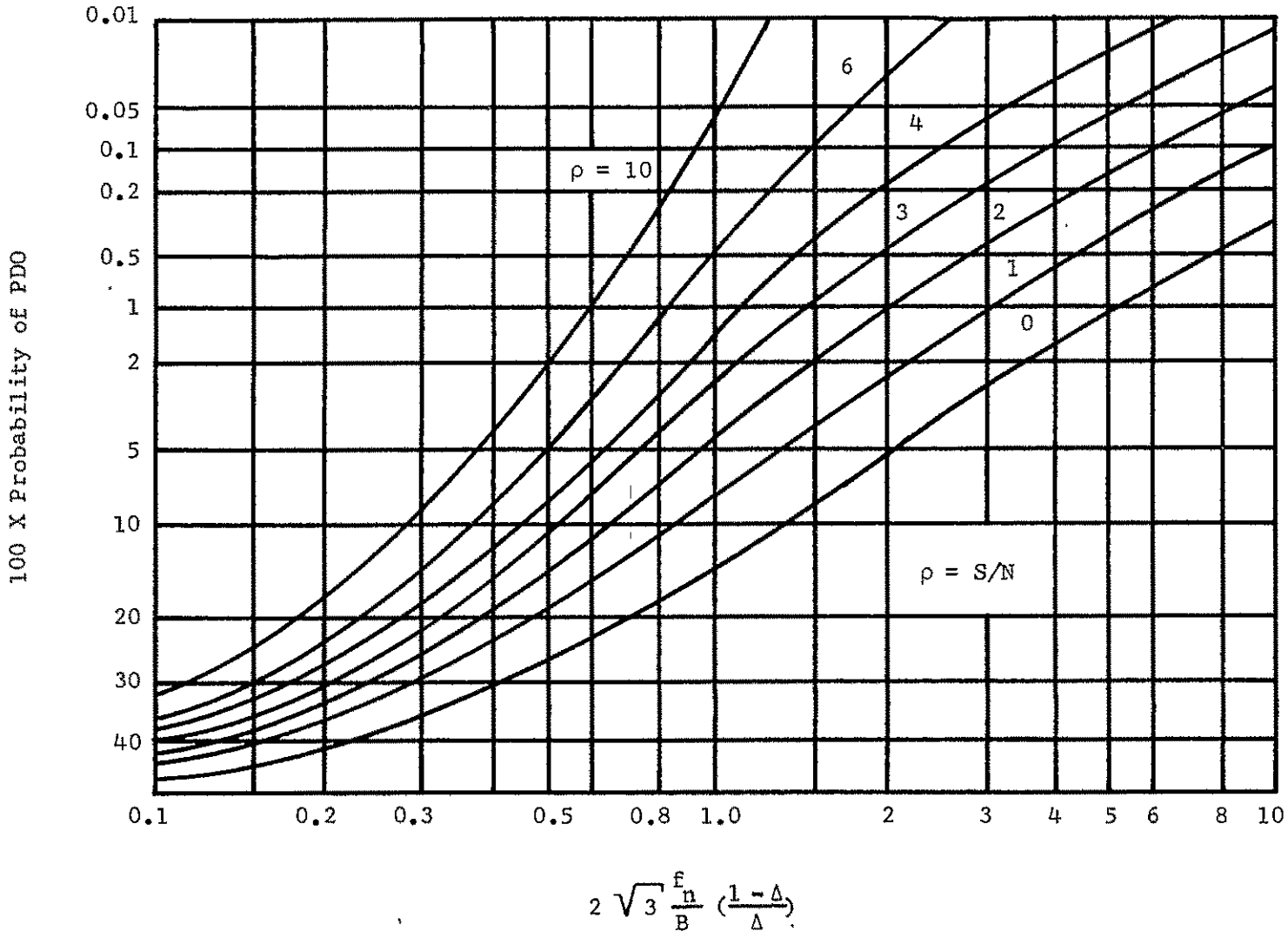

Figure 4-5 PDO Distribution Function

channels. The effect on such channels is illustrated in Figure 4-6 for a data channel having a bandwidth of 3 kHz and a carrier of 15 kHz. As the signal-to-noise ratio and the channel carrier frequency increase, the effect becomes negligible.

C. Monostable Multivibrator Perturbations Due to Flutter

In the preceding section it was shown that MSMV pulse dropout occurred when additive noise deviated the carrier frequency by an amount such that the distance between adjacent carrier zero crossings is less than the MSMV "on" time. Since flutter also results in such deviations, there is a possibility of pulse dropout due to flutter. The work which follows proves that the probability of this occurrence is negligibly small.

The analysis will be performed by assuming flutter to have a Gaussian distribution of zero mean, an assumption supported by experimental evidence.[10] The frequency deviation of a frequency ω_n, due to flutter, can be written as

$$\dot{\theta}(t) = \omega_n g(t) \tag{4.15}$$

where $\dot{\theta}(t)$ and $g(t)$ represent frequency deviation and flutter, respectively. If a 3σ approximation is employed to relate the peak and rms values of $\dot{\theta}(t)$, the result is

$$3\sigma = \dot{\theta}_{peak} = \omega_n \, g_{peak} , \tag{4.16}$$

where σ represents the rms value of $\dot{\theta}(t)$, and $\dot{\theta}_{peak}$ and g_{peak} represent the peak values of $\dot{\theta}(t)$ and $g(t)$, respectively. As before, P(PDO) is given by

$$P(PDO) = P(\dot{\theta} \geq \omega_n \frac{1 - \Delta}{\Delta}) , \tag{4.17}$$

or, since $p(\dot{\theta})$ is assumed Gaussian with zero mean

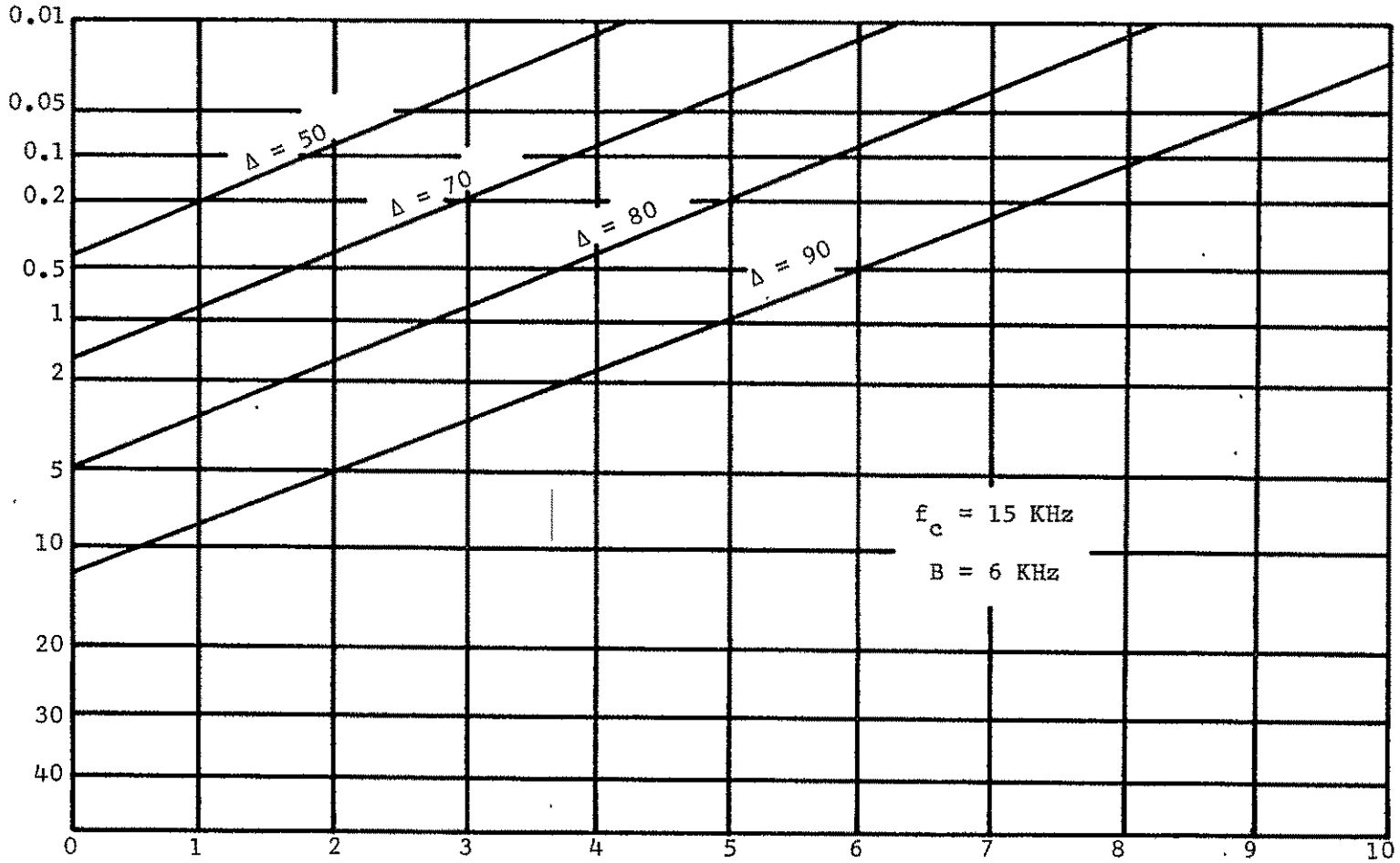

Figure 4-6 Probability of PDO for a Low Frequency Channel

$$P(PDO) = \frac{1}{\sqrt{2\pi}\sigma} \int_{\omega_n(\frac{1-\Delta}{\Delta})}^{\infty} e^{-y^2/2\sigma^2} dy \tag{4.18}$$

This equation is equivalent to

$$P(PDO) = \frac{1}{2} - \frac{1}{\sqrt{2\pi}\sigma} \int_{o}^{\omega_n(\frac{1-\Delta}{\Delta})} e^{-y^2/2\sigma^2} dy \tag{4.19}$$

If the preceding is placed into the form of a normal distribution, the result is

$$P(PDO) = \frac{1}{2} - \frac{1}{\sqrt{2\pi}} \int_{o}^{\xi} e^{-x^2/2} dx \ , \tag{4.20}$$

where

$$\xi = \frac{\omega_n}{\sigma} (\frac{1-\Delta}{\Delta}) \ . \tag{4.21}$$

The expression for P(PDO) may be placed in terms of flutter by substituting (4.16) into (4.21) to yield

$$\xi = \frac{3}{g_{peak}} (\frac{1-\Delta}{\Delta}) \ . \tag{4.22}$$

In order to show that P(PDO) is negligible, choose $\Delta = 0.9$ and $g_{peak} = 0.01$. These values yield $\xi = 33.3$, which when substituted into (4.22) illustrates that P(PDO) is negligible. Values of Δ less than 0.9 and values of g_{peak} less than 0.01, as would certainly be the case for a good recorder, would yield a still larger value of ξ and consequently a smaller P(PDO).

D. Phase-Lock Loop Perturbations Due to Channel Noise

Noise which falls within the channel bandwidth perturbs the carrier phase and affects the stability of the demodulation carrier. Since the output of the channel filter is limited, only phase perturbations are of

interest. The phase perturbations of the channel zero crossings have an approximate Gaussian density function for high signal-to-noise ratios and the rms value of these perturbations is given by[11]

$$\sigma_\phi = \frac{1}{\sqrt{2\ S/N}} \quad , \tag{4.25}$$

where S/N represents the average signal-to-noise ratio in the data channel. Equation (4.25) is plotted in Figure 4-7.

The rms value of phase jitter on the PLL output is less than that given by (4.25) because of the additional band-limiting action of the PLL. The variance of the PLL output may be written as

$$\sigma_{out}^2 = \frac{\sigma_{in}^2}{B} \int_0^\infty \left| H(\omega) \right|^2 \frac{d\omega}{2\pi} \quad , \tag{2.26}$$

where σ_{out}^2 and σ_{in}^2 represent the phase variances of the PLL output and input, $H(\omega)$ is the PLL transfer function, and B is the input noise bandwidth. The integral is simply the noise bandwidth of the PLL.[12] Equation (2.26) is valid only for the case where the noise bandwidth of the PLL is less than B. If the noise bandwidth of the PLL is greater than B, σ_{out}^2 and σ_{in}^2 are approximately equal.

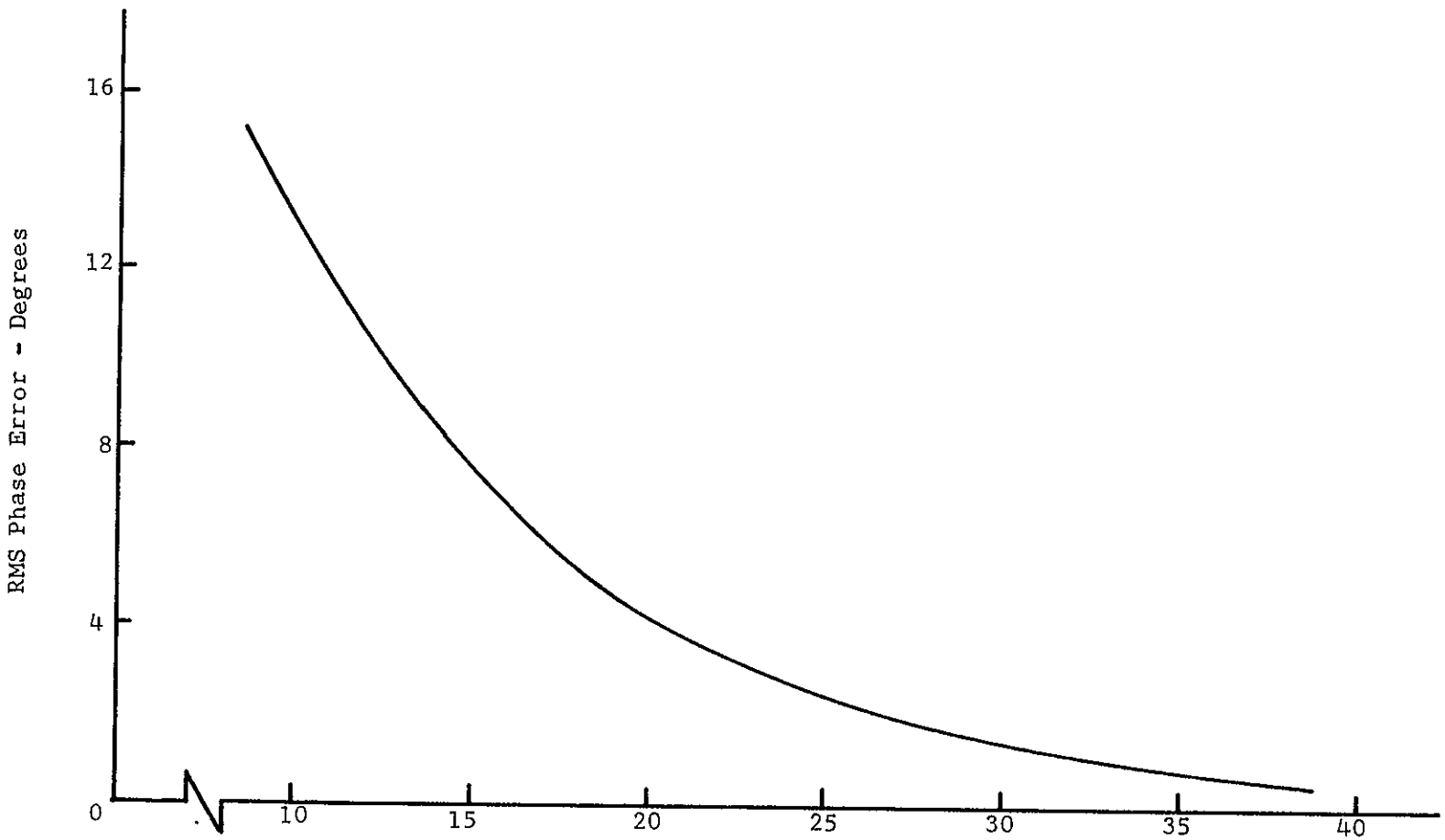

Figure 4-7. RMS Phase Perturbation Due to Noise

V. SUMMARY

There are several methods of performing carrier synthesis from modulated carriers, all of which are valid only for DSB signals. If SSB or QDSB signals are to be demodulated, then the demodulation carrier must be derived from some other source, such as from a pilot.

In the carrier synthesis system which utilizes a limiter and a monostable multivibrator, perturbations result from modulation zeros, flutter and noise. Modulation zeros cause perturbations in the form of shifted pulses in the MSMV output, which yield phase errors in the demodulation carrier. The analysis illustrates that this effect is worst on low-frequency, wideband channels. The probability of a shifted pulse is probably negligible if the carrier frequency is five times the bandwidth of the data signal and if the MSMV duty is 70 percent or greater. For a carrier frequency greater than 15 kHz the phase-lock loop response is negligible if the bandwidth of the phase-lock loop is made only large enough for flutter compensation.

For low signal-to-noise ratios problems arise because of excessive phase jitter in the synthesized demodulation carrier and because of pulse dropout in the MSMV output. The first problem appears negligible for a signal-to-noise ratio greater than 20 db. Pulse dropout is more difficult to specify because it depends upon the channel carrier frequency, the MSMV duty cycle, and the channel bandwidth, as well as the signal-to-noise ratio. The analysis shows that for 3 kHz channels the pulse dropout problem appears negligible for a channel carrier frequency greater than 15 db. For practical signal-to-noise ratios this effect is negligible for a 50 percent duty cycle MSMV.

Pulse dropout due to flutter is also a negligible effect. However, tape recorder flutter, even if perfectly tracked by the phase-lock loop, yields phase perturbations as high as 10 degrees on a demodulated 3 kHz sinusoid. The need for recorders with a low peak TBE is evident.

APPENDIX

PHASE-LOCK-LOOPS

Phase-lock loops are covered in considerable detail in the literature, and the book by Gardner[13] contains an extensive bibliography. Thus, a complete exposition of the area is not the purpose of this appendix. Instead, the purpose here is only to develop the step phase response needed in Chapter IV.

A. The Linear Model

A block diagram of the PLL is illustrated in Figure A-1(a). The output of the phase comparator is a voltage proportional to the phase difference between the input signal and the VCO signal. This signal is then amplified and filtered by the loop filter. The output of the loop filter drives the VCO in such a manner as to minimize the phase error between the input signal and the VCO output signal.

In order to better understand the operation of the PLL, let the input signal be

$$e_{in}(t) = \sin\left[\omega t + \theta_i(t)\right] \tag{A.1}$$

and assume the VCO output to be

$$e_{VCO}(t) = \cos\left[\omega t + \theta_o(t)\right] \tag{A.2}$$

The phase detector output can be written as

$$e_\phi(t) = K_d\, e_i(t)\, e_o(t) \tag{A.3}$$

where K_d is a constant having units of volts per radian. Substituting (A.1) and (A.2) into (A.3) yields

$$e_\phi(t) = K_d \sin\left[\theta_i(t) - \theta_o(t)\right] \tag{A.4}$$

plus a high frequency (2ω) term, which need not be considered because it will not be passed by the loop filter. If the phase error function, $\theta_e(t)$, defined as

$$\theta_e(t) = \theta_i(t) - \theta_o(t) \tag{A.5}$$

is small, the output of the phase detector can be written as

$$e_\phi(t) = K_d\ \theta_e(t) \tag{A.6}$$

The voltage, $e_\phi(t)$, is amplified and filtered by the loop filter to yield the VCO input voltage. The VCO output frequency deviation, $\dot{\theta}_o(t)$, is proportional to the input voltage, or

$$\dot{\theta}_o(t) = K_{VCO}\ e_v(t) \tag{A.7}$$

where K_{VCO} is a constant associated with the VCO. Upon taking the Laplace transform, (A.7) can be written as

$$\theta_o(S) = \frac{1}{S} K_{VCO}\ E_v(S) \tag{A.8}$$

The foregoing discussion leads to the linear model of the PLL illustrated in Figure A-1(b). The input and output are now the phase deviations of the actual input and output. The gains of the various loop elements are lumped together to form the total loop gain, A, defined by

$$A = K_d\ K_{VCO}\ A_L \tag{A.9}$$

where A_L is the gain of the loop amplifier.

The transfer function relating $\theta_i(S)$ and $\theta_o(S)$ can be written as

$$\frac{\theta_o(S)}{\theta_i(S)} = \frac{AF(S)}{S + AF(S)} \tag{A.10}$$

The assumption will now be made that the loop is the "perfect" second-order type, for which

$$F(S) = \frac{S + a}{S} \tag{A.11}$$

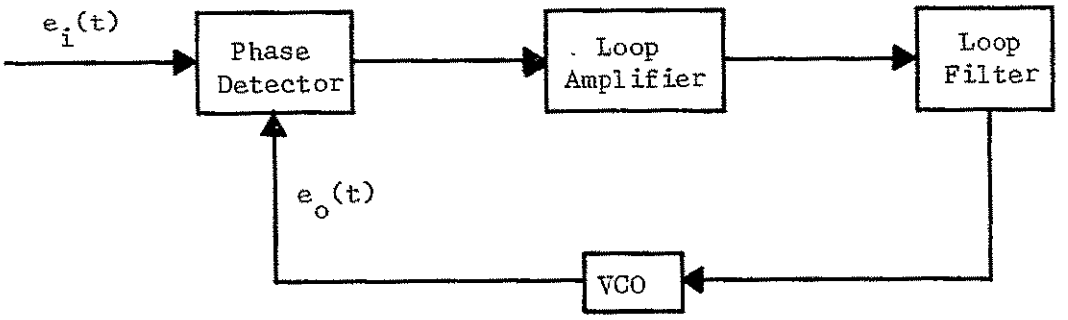

(a) Phase Lock Loop

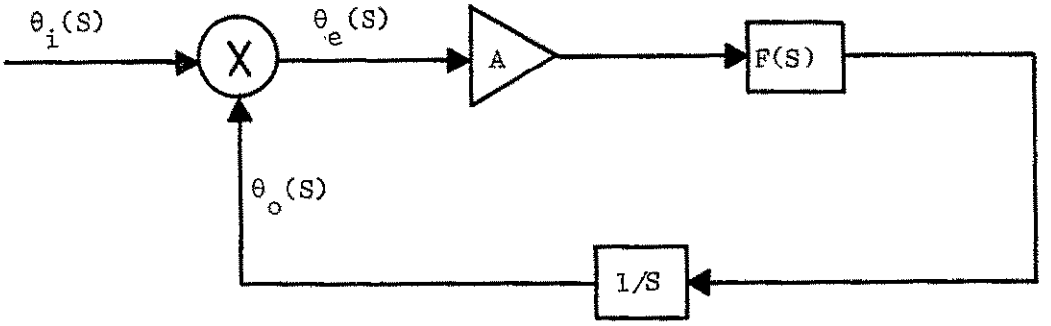

(b) Linear Model of the PLL

Figure A-1 Phase-Lock Loop and the Linear Model

The word "perfect" refers to the integration, which is easily implemented using an active realization. Substitution of (A.11) into (A.10) yields

$$\frac{\theta_o(S)}{\theta_i(S)} = \frac{A(S+a)}{S^2 + A(S+a)} \tag{A.12}$$

which can be placed into the familiar second order form,

$$\frac{\theta_o(S)}{\theta_i(S)} = \frac{2\zeta\omega_N S + \omega_N^2}{S^2 + 2\zeta\omega_N S + \omega_N^2} \tag{A.13}$$

by letting

$$\omega_N = \sqrt{Aa} \tag{A.14}$$

and

$$\zeta = \frac{1}{2}\sqrt{\frac{A}{a}} \tag{A.15}$$

The parameters ζ and ω_N are known as the loop damping and the loop natural frequency, respectively, and can be implemented by properly choosing the loop filter parameter, a, and the loop gain, A.

B. Response to Phase-Step

From (A.13) the response to a phase step may be determined. For simplicity the loop phase error will be determined using

$$\theta_e(S) = \frac{S^2}{S^2 + \zeta\omega_N S + \omega_N^2}\,\theta_i(S) \ , \tag{A.16}$$

and then $\theta_o(t)$ may be found by

$$\theta_o(t) = \theta_i(t) - \theta_e(t) \tag{A.17}$$

Let the magnitude of the step be K_p radians. Then

$$\theta_e(t) = K_p\, L^{-1}\left[\frac{S}{S^2 + 2\zeta\omega_N S + \omega_N^2}\right] \tag{A.18}$$

where L^{-1} represents the inverse Laplace transform. Performing this operation yields

$$\theta_e(t) = K_p \left[\cos \omega_N \sqrt{1-\zeta^2}\, t - \frac{\zeta}{\sqrt{1-\zeta^2}} \sin \omega_N \sqrt{1-\zeta^2}\, t \right] e^{-\zeta\omega_N t} \qquad (A.19)$$

or

$$\theta_o(t) = K_p \left[1 - e^{-\zeta\omega_N t} \left[\cos \omega_N \sqrt{1-\zeta^2}\, t - \frac{\zeta}{\sqrt{1-\zeta^2}} \sin \omega_N \sqrt{1-\zeta^2}\, t \right] \right], \qquad (A.20)$$

The phase error, $\theta_e(t)$, is illustrated in Figure A-2 for two values of ζ and a normalized ω_N. Also plotted in A-2 is the function

$$\theta_m = e^{-\zeta\omega_N t} \qquad (A.21)$$

It is clear from the figure that $\theta_m(t)$ is a good approximation of the envelope of $\theta_e(t)$. Thus, $1 - \theta_m(t)$ can be used as an approximation of $\theta_o(t)$ with reasonable accuracy. This is done in Chapter IV.

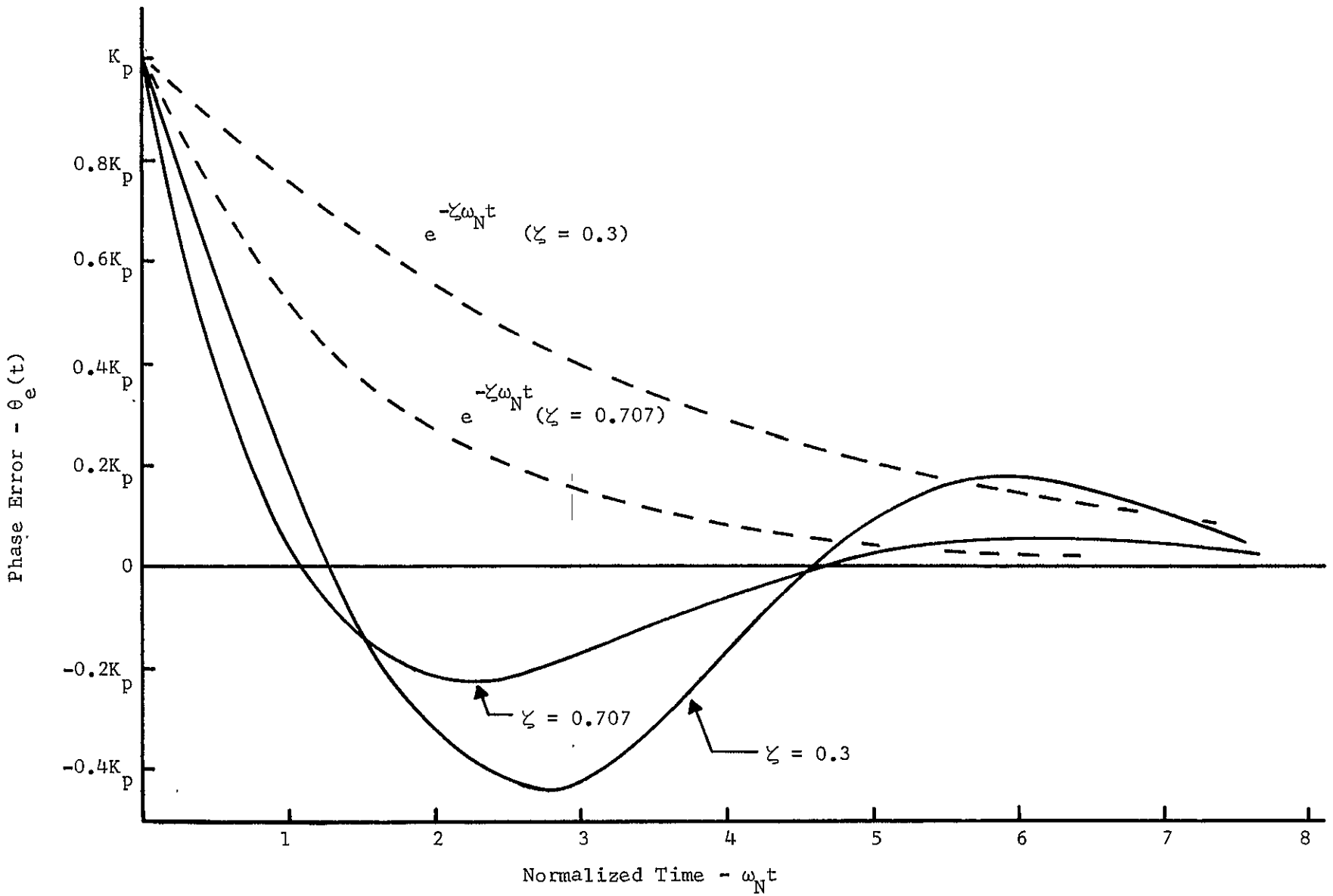

Figure A-2 Phase-Lock Loop Response to a Phase Step

REFERENCES

1. Simpson, R. S., and Tranter, W. H., "AM-Baseband Telemetry Systems, Vol. 1: Factors Affecting A Common Pilot System," University of Alabama, Bureau of Engineering Research, February, 1968.

2. Costas, J. P., "Synchronous Communications," Proceedings of the IRE, Vol. 44, No. 12, December, 1965, pp. 1713-1718.

3. Roche, A. O., "The Use of Double Sideband Suppressed Carrier Modulation as a Subcarrier for Vibration Telemetry," Proceedings of the National Telemetering Conference, June, 1964, paper 5-3.

4. Payne, R. C., "DSB and its Utilization in Telemetry Systems," Proceedings of the National Telemetering Conference, April, 1965, pp. 160-163.

5. Simpson, R. S., and Tranter, W. H., "Carrier Synthesis from Perturbed DSB/SC Signals," Proceedings of the International Telemetering Conference, Vol. 3, October, 1967, pp. 371-381.

6. Simpson, R. S., and Tranter, W. H., "Effect of Recorder Time-Base Error on an AM-Baseband Telemetry System," IEEE Transactions on Communication Technology, Vol. COM-16, No. 2, April, 1968, pp. 316-320.

7. Schwartz, M., Bennett, W. R., and Stein, S., Communication Systems and Techniques, McGraw-Hill Book Company, Inc., New York, 1966, pp. 229-232.

8. Rice, S. O., "Mathematical Analysis of Random Noise," Bell System Technical Journal, Vol. 24, No. 1, January, 1945, p. 55.

9. Rice, S. O., "Statistical Properties of a Sine Wave Plus Random Noise," Bell System Technical Journal, Vol. 27, No. 1, January, 1948, p. 120.

10. Chao, S. C., "Flutter and Time Errors in Magnetic Data Recorders," Proceedings of the International Telemetering Conference, Vol. 1, May, 1965, pp. 578-594.

11. Panter, Philip F., Modulation, Noise and Spectral Analysis, McGraw-Hill Book Company, Inc., New York, 1966, p. 35

12. Viterbi, Andrew J., Principles of Coherent Communication, McGraw-Hill Book Company, Inc., New York, 1966, p. 35.

13. Gardner, F. M., Phaselock Techniques, John Wiley and Sons, Inc., New York, 1966.

BIBLIOGRAPHY

BOOKS

Bennett, W. R., and Davy, J. R., Data Transmission, McGraw-Hill Book Company, Inc., New York, 1965.

Davenport, Wilber B., Jr., and Root, William L., An Introduction to the Theory of Random Signals and Noise, McGraw-Hill Book Company, Inc., New York, 1958.

Davies, Gomer L., Magnetic Tape Instrumentation, McGraw-Hill Book Company, Inc., New York, 1961.

Gardner, F. M., Phaselock Techniques, John Wiley and Sons, Inc., New York, 1966.

Hancock, J. C., An Introduction to the Principles of Communication Theory, McGraw-Hill Book Company, Inc., New York, 1961.

Harman, Willis W., Principles of the Statistical Theory of Communication, McGraw-Hill Book Company, Inc., New York, 1963.

Panter, Philip F., Modulation, Noise, and Spectral Analysis, McGraw-Hill Book Company, Inc., New York, 1965.

Papoulis, A., Probability, Random Variables, and Stochastic Processes, McGraw-Hill Book Company, Inc., New York, 1965.

Rowe, Harrison E., Signals and Noise in Communication Systems, D. Van Nostrand Company, Inc., Princeton, New Jersey, 1965.

Schwartz, M., Bennett, W. R., and Stein, S., Communication Systems and Techniques, McGraw-Hill Book Company, Inc., New York, 1966.

Viterbi, Andrew J., Principles of Coherent Communication, McGraw-Hill Book Company, Inc., New York, 1966.

ARTICLES, REPORTS, AND PAPERS

Bagdady, Elie, J., "Theory of Low-Distortion Reproduction of FM Signals in Linear Systems," IRE Transactions on Circuit Theory, Vol. CT-5.

Carson, J. R., and Fry, T. C., "Variable-Frequency Electric Circuit Theory," Bell System Technical Journal, Vol. 16, pp. 513-540, October, 1937.

Chao, S. C., "Flutter and Time Errors in Magnetic Data Recorders," Proceedings of the International Telemetering Conference, Vol. 1, pp. 578-594, May, 1965.

Costas, J. P., "Synchronous Communications," Proceedings of the IRE, Vol. 44, No. 12, pp. 1713-1718, December, 1956.

Morley, G. A., "Phase Delay Variations in an FM Receiver," Canadian Armament Research and Development Establishment Technical Memorandum 344/60, July, 1960.

Nichols, M. H., "Some Analysis of the WSMR Test Results on DSB," Proceedings of the International Telemetering Conference, Vol. 3, pp. 361-370, October, 1967.

Nichols, M. H., and Rauch, L. L., "Telemetry," USAF Report No. ESD-TR-66-464 July, 1966.

Payne, R. C., "DSB and Its Utilization in Telemetry Systems," Proceedings of the National Telemetering Conference, pp. 160-163, April, 1965.

Ratz, Alfred G., "The Effect of Tape Transport Flutter on Spectrum and Correlation Analysis," IEEE Transactions on Space Electronics and Telemetry, Vol. SET-10, pp. 129-134, December, 1964.

Rice, S. O., "Mathematical Analysis of Random Noise," Bell System Technical Journal, Vol. 23, pp. 282-332, July, 1944.

Rice, S. O., "Statistical Properties of Sine Wave Plus Random Noise," Bell System Technical Journal, Vol. 27, pp. 109-157, January, 1948.

Roach, A. O., "The Use of Double Sideband Suppressed Carrier Modulation as a Subcarrier for Vibration Telemetry," Proceedings of the National Telemetering Conference, paper 5-3, June, 1964.

Schmitt, F. J., "Double Sideband Suppressed Carrier Telemetry System," Proceedings of the International Telemetering Conference, Vol. 3, pp. 347-360, October, 1967.

Simpson, R. S., and Davis, R. C., "Tape Recorder Flutter Analysis and Bit-Rate Smoothing of Digital Data," University of Alabama, Bureau of Engineering Research, June, 1966.

Simpson, R. S., and Tranter, W. H., "Effect of Recorder Flutter on Coherent Demodulation in an AM-Baseband System," Proceedings of the National Telemetering Conference, pp. 46-49, May, 1967.

Simpson, R. S., and Tranter, W. H., "Carrier Synthesis from Perturbed DSB/SC Signals," Proceedings of the International Telemetering Conference, Vol. 3, pp. 371-381, October, 1967.

Simpson, R. S., and Tranter, W. H., "AM-Baseband Telemetry Systems, Vol. 1: Factors Affecting a Common Pilot System," University of Alabama, Bureau of Engineering Research, February, 1968.

Simpson, R. S., and Tranter, W. H., "Effect of Recorder Time-Base Error on an AM-Baseband Telemetry System," IEEE Transactions on Communication Technology, Vol. COM-16, No. 2, pp. 316-320, April, 1968.

Van der Pol, B., "The Fundamental Principles of Frequency Modulation," Journal of the Institution of Electrical Engineers, Vol. 93, Part III, pp. 153-158, May, 1946.

COMMUNICATION SYSTEMS GROUP

RECENT REPORTS

An Exponential Digital Filter for Real Time Use, R. S. Simpson, C. A. Blackwell and W. H. Tranter, July, 1965.

An Evaluation of Possible Modifications of the Existing IRIG FM/FM Telemetry Standards, R. S. Simpson, C. A. Blackwell and J. B. Cain, May, 1966.

Analysis of Premodulation Gain in a SS/FM Telemetry System, R. S. Simpson and C. A. Blackwell, June, 1966.

Tape Recorder Flutter Analysis and Bit-Rate Smoothing of Digital Data, R. S. Simpson and R. C. Davis, June, 1966.

A Study of Redundancy in Saturn Flight Data, R. S. Simpson and J. R. Haskew, August, 1966.

AM-Baseband Telemetry Systems, Vol. 1: Factors Affecting a Common Pilot System, R. S. Simpson and W. H. Tranter, February, 1968.

Waveform Distortion in an FM/FM Telemetry System, R. S. Simpson, R. C. Houts and F. D. Parsons, June, 1968.

A Digital Technique to Compensate for Time-Base Error in Magnetic Tape Recording, R. S. Simpson, R. C. Houts and D. W. Burlage, August, 1968.

A Study of Major Coding Techniques for Digital Communication, R. S. Simpson and J. B. Cain, January, 1969.

AM-Baseband Telemetry Systems, Vol. 2: Carrier Synthesis from AM Modulated Carriers, R. S. Simpson and W. H. Tranter, June, 1969.